August 2021

Negative Regulation of the Kinase LIN-45 By the E3/E4 Ubiquitin Ligase UFD-2

Augustin Deniaud
University of Wisconsin-Milwaukee

NEGATIVE REGULATION OF THE KINASE LIN-45 BY THE E3/E4 UBIQUITIN LIGASE UFD-2

by

Augustin Deniaud

A Thesis Submitted in

Partial Fulfillment of the

Requirements for the Degree of

Master of Science

in Biological Sciences

at

The University of Wisconsin-Milwaukee

August 2021

ABSTRACT

NEGATIVE REGULATION OF THE KINASE LIN-45 BY THE E3/E4 UBIQUITIN LIGASE UFD-2

by

Augustin Deniaud

The University of Wisconsin-Milwaukee, 2021
Under the Supervision of Professor Claire de la Cova

The serine/threonine kinase BRAF is a key part of the Ras-Raf-MEK-ERK pathway, an inducer of cell growth, differentiation, and survival. In humans, activating mutations, most commonly BRAF(V600E), have been detected in several cancers, including melanoma and thyroid cancer. In the *Caenorhabditis elegans* ortholog LIN-45, the equivalent mutation LIN-45(V627E) results in elevated Raf-MEK-ERK signaling. We performed an unbiased genetic screen to identify negative regulators of LIN-45(V627E). Here, we report the identification of the E3/E4 ubiquitin ligase UFD-2, and show it is a negative regulator of LIN-45 protein activity and levels. Loss of UFD-2 leads to accumulation of wild-type LIN-45 protein as well as LIN-45(V627E). Based on analysis of truncations in the LIN-45 protein and mutations in the conserved 14-3-3 sites, we propose a model where UFD-2-dependent regulation requires binding by 14-3-3 proteins. This contrasts with the previously characterized degradation of LIN-45 by the E3 ubiquitin ligase SEL-10, which only requires a minimal phospho-degron sequence. We also identify the AAA ATPase CDC-48.1/2, a known interactor of UFD-2, as a negative regulator of LIN-45 protein stability. These findings represent a previously

unrecognized mechanism of Ras-Raf-MEK-ERK regulation and will be the basis of future investigations of ubiquitin-mediated degradation of Raf.

TABLE OF CONTENTS

LIST OF FIGURES

LIST OF TABLES

ACKNOWLEDGEMENTS

Thank you to my mentors Claire de la Cova and Robert Townley for their patience, passion, knowledge, wisdom, and encouragement.

Thank you to my committee members, Jennifer Gutzman and Christopher Quinn, for their guidance and support.

Lastly, thank you to my wife, family, and friends for all their support.

CHAPTER 1 - INTRODUCTION

BRAF's role in melanoma

Melanoma is a malignant tumor developed from melanocytes, typically caused by UV exposure. It is the deadliest form of skin cancers, accounting for an estimated 100,350 cases and 6,850 deaths in 2020 (Siegel, Miller, & Jemal 2020). Annual treatment costs are predicted to increase to $1.6 billion by 2030 (Guy et al., 2015).

In humans, mutations in the gene *BRAF* have been detected in certain cancers, including 70% of melanomas and 30-50% of thyroid cancers (Mercer et al., 2009). BRAF is a member of the Raf family of proteins kinases. It is activated by GTP-bound Ras, and in turn activates the kinases MEK and ERK, referred to here as the Ras-Raf-MEK-ERK pathway. In particular, the V600E in BRAF causes constitutive activity of the BRAF protein kinase and accounts for more than 80% of mutations in BRAF (Davies et al., 2002). This mutation induces similar conformation changes to activating phosphorylations at T599 and S602, leading to constitutive BRAF activity without the requirement for upstream pathway activation (Köhler & Brummer 2016).

C. elegans as a model organism

The roundworm *Caenorhabditis elegans* is a powerful model in which to study mechanisms of animal development (Kaletta & Hengartner, 2006). Once an egg is laid, an individual passes through several larval molts, termed L1-L4, before developing into a fertile adult. Due to its invariant cell lineage and fully characterized cells and tissues, developmental events occur in the same way in each individual. *C. elegans* is

transparent, enabling the use of fluorescent transgenes to characterize gene expression. Tools for genetic manipulation are already well-characterized, including robust RNAi screening protocols (Conte et al., 2015) and transgenesis using the CRISPR/Cas9 system (Dickinson & Goldstein, 2016) or transposon insertion (Frøkjaer-Jensen et al., 2014). Finally, the *C. elegans* genome is fully sequenced and conserved, with approximately 41% of *C. elegans* genes having human orthologs (Kim et al., 2018).

Ras signaling in C. elegans

Signaling through the Ras-Raf-MEK-ERK signaling pathway in *C. elegans* has diverse roles in many cellular processes, such as germline development, organogenesis, axon outgrowth, and cell fate specification (Sundaram 2013), and is strongly conserved throughout animal evolution (Fig. 1). Several key portions of Ras signaling were first identified in *C. elegans*, including the placement of Ras upstream of Raf (Han et al., 1993) and the identification of pathway components such as Grb2/SEM-5 (Clark et al., 1992). Ras signaling is required for proper specification of cell fates in the male spicule, excretory duct cell, and vulval precursor cells. Hyperactivation of Ras signaling in the vulval precursor cells causes ectopic vulval development, termed the Muv phenotype (Ferguson & Horvitz 1985).

Regulation of the Ras-Raf-MEK-ERK pathway

Activation of the Ras-Raf-MEK-ERK pathway can occur due to various stimuli, such as cellular stress and growth factor reception, notably extracellular growth factor (EGF) binding to its receptor, the receptor tyrosine kinase (RTK) family member EGFR. The mechanisms of signal transduction are well conserved; for each factor, we reference

both human and *C. elegans* proteins. The *C. elegans* Ras ortholog LET-60 is part of a family of small GTPases involved in the transmission of extracellular signals leading to cell growth and development (Sundaram 2013). Activation of the RTK LET-23 causes recruitment of the Grb2/SOS(SEM-5/SOS-1) complex and recruitment to the plasma membrane where LET-60 is localized. The guanine nucleotide exchange factor SOS-1 stimulates the release of GDP from LET-60, promoting formation of its active GTP-bound state (Karnoub and Weinberg 2008). In its GTP-bound state, LET-60 recruits the BRAF ortholog LIN-45 to the plasma membrane (Udell et al., 2011). A phosphorylation cascade then occurs, where LIN-45 phosphorylates its substrate, the MAPKK family kinase MEK/MEK-2. MEK-2 phosphorylates its substrate, the MAPK family kinase ERK/MPK-1, and MPK-1 goes on to phosphorylate a wide range of substrates in the cytoplasm and nucleus, leading to downstream cellular processes (Yoon & Seger 2006).

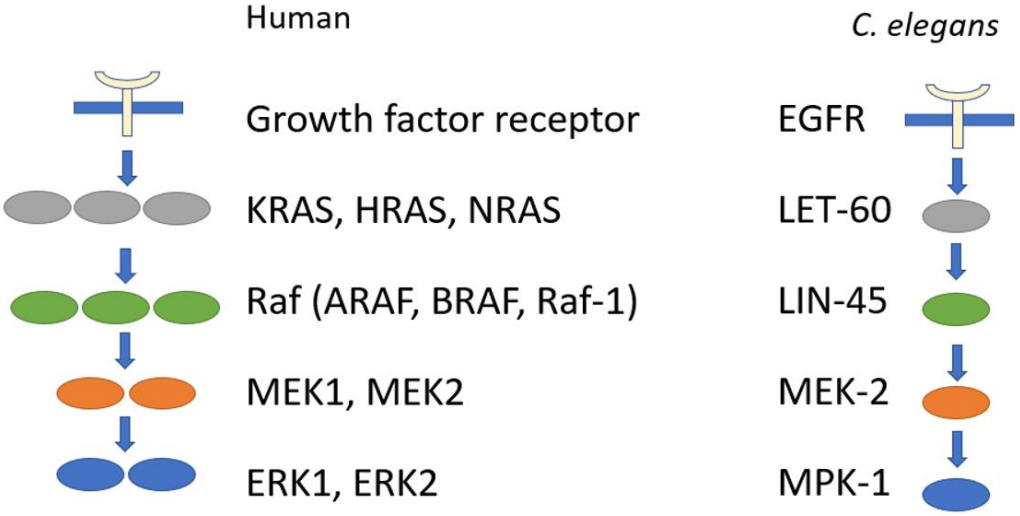

Figure 1.1. Conservation of the Ras-Raf-MEK-ERK pathway. Humans have several orthologs of each protein in the pathway: three Ras orthologs (KRAS, HRAS, NRAS), three Raf orthologs (ARAF, BRAF, CRAF/RAF1), two MEK orthologs (MEK1, MEK2), and two ERK orthologs (ERK1, ERK2). In comparison, the pathway in C. elegans is simpler, with only one ortholog of each: LET-60(Ras), LIN-45(Raf), MEK-2(MEK), and MPK-1(ERK).

Regulation of BRAF activation is controlled through several steps (Lavoie & Therrien 2015). Inactive BRAF exists in the cytosol in an auto-inhibited state in a complex with 14-3-3 proteins bound to phosphorylated S365 (Muslin et al. 1996). Once Ras is activated, it binds to BRAF through the Ras-binding domain (RBD) and cysteine-rich domain (CRD) region, recruiting BRAF to the plasma membrane. This step includes dephosphorylation of S365, release of the 14-3-3, and relieving of the auto-inhibition (Dhillon et al. 2002). BRAF is then phosphorylated several times, and finally dimerizes with the assistance of 14-3-3 proteins (Garnett et al., 2005, Rushworth et al., 2006). Phosphorylation of T599 and S602 leads to opening of an inhibitory loop in the catalytic cleft of BRAF and is required for kinase activation. The oncogenic V600E mutation mimics the phosphorylation of these residues in that it also results in opening of the inhibitory loop (Kiel et al., 2016).

LIN-45 sequence, regulation, and activity is strongly conserved from *C. elegans* to human. Sequence similarity is high (Appendix A), especially in the RBD, CRD, and kinase domain, which are highly conserved among all Raf family members (Han et al., 1993). LIN-45 regulation is also conserved, as LET-60 binding, 14-3-3 binding, and kinase activity were found to be necessary for full LIN-45 function (Hsu et al., 2001). Activation of LIN-45 through phosphorylation of residues at the activation loop site is also conserved, as mutations of these residues to phosphomimetic residues was enough to cause constitutive kinase activity in both worm and human models (Chong, Lee, & Guan 2001, de la Cova & Greenwald 2012).

The role of the Ras-Raf-MEK-ERK pathway in vulval development of C. elegans

In *C. elegans*, the Ras-Raf-MEK-ERK pathway is important in cell fate specification during vulval development (Shin & Reiner, 2018). The *C. elegans* vulva arises from six vulval precursor cells (VPCs) named P3.p-P8.p (Fig. 2). Each VPC can adopt primary, secondary, or tertiary fate depending on the signaling it receives. During normal development, the nearby anchor cell (AC) releases epidermal growth factor(EGF), which activates the Ras-Raf-MEK-ERK pathway in the closest VPC, P6.p. This results in induction of primary fate in P6.p, which undergoes several cell divisions to develop into the central structures of the vulva. One substrate of ERK in VPCs is the transcription factor and repressor Elk1/LIN-1. Phosphorylation of LIN-1 relieves repression of its target genes and results in transcription of the DSL/Notch ligand LAG-2 (Zhang & Greenwald 2011). LAG-2 then activates the Notch pathway in the adjacent VPCs P5.p and P7.p, resulting in secondary fate specification in these VPCs and further cell divisions that lead to development into the side structures of the vulva. Activation of the Notch pathway also suppresses primary fate specification. VPCs that receive neither the primary nor secondary fate signals adopt tertiary fate and fuse with the hypodermis.

The Ras-Raf-MEK-ERK pathway can become hyperactivated through mechanisms such as mutations that hyperactivate Ras, mutations that hyperactivate Raf, or the loss of a negative regulator (Schubbert, Shannon & Bollag 2007). Hyperactivation of the pathway in VPCs results in ectopic primary fate specification and the development of pseudovulval structures, termed the Muv phenotype. Introduction of a transgene expressing LIN-45(V627E) only results in a mild Muv phenotype (de la Cova &

Greenwald, 2012). Loss of negative regulators, including the genes *sel-10*, *gsk-3*, and *cdk-2* further described below, enhances the Muv phenotype resulting from LIN-45(V627E) (de la Cova & Greenwald, 2012; de la Cova et al., 2020).

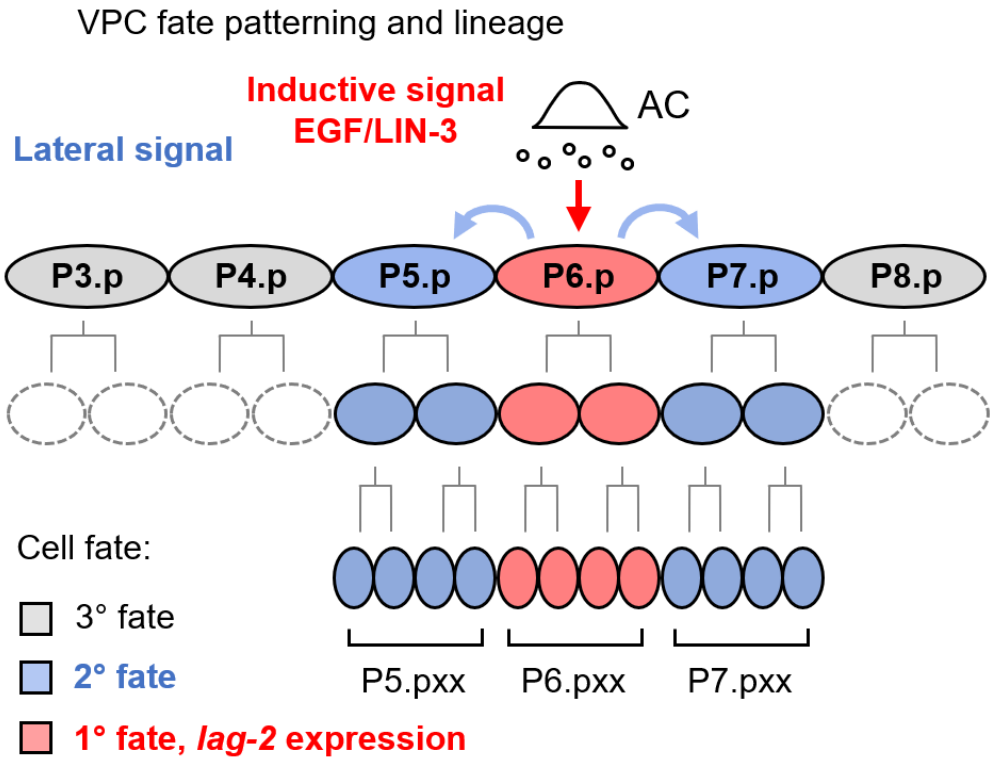

Figure 1.2. The patterning of VPC fates and lineages in the development of the C. elegans vulva. The inductive signal EGF/LIN-3 is released by the anchor cell (AC). The nearest VPC to the AC, P6.p, receives the signal and activates the Ras-Raf-MEK-ERK pathway. This activation causes P6.p to adopt primary fate (1°). Activation also causes expression of the lateral signal, activating the Notch pathway in adjacent VPCs (P5.p and P7.p). This activation causes these VPCs to adopt secondary fate (2°). Cells which receive neither signal adopt tertiary fate (3°) and fuse with the hypodermis.

The ubiquitin-proteasome system

The ubiquitin-proteasome system is a major regulator of protein levels through ubiquitin-mediated proteolysis. In this system, proteins are modified by the covalent addition of the small protein ubiquitin. The enzymes that perform this modification are classified into E1, E2, E3, and E4 ubiquitin ligases (Papaevgeniou & Chondrogianni 2014).

Ubiquitin is first activated by an E1 category enzyme. Ubiquitin is then passed to an E2 conjugating enzyme. A substrate-specific E3 ligase recruits its target and mediates the passing of ubiquitin from the E2 to the substrate. Additional ubiquitin peptides are then added to the present ubiquitin by either E3 or E4 ubiquitin ligases. E3 ligases are capable of mono- or poly-ubiquitination, but E4 ligases are only capable of poly-ubiquitination. There exist several classes of E3 and E4 ligases, including U-box domain proteins, monomeric RING finger proteins, and multisubunit RING finger complexes (Passmore & Barford 2004).

Once modified with poly-ubiquitin chains, proteins are recognized as substrates for the 26S proteasome, a large cylindrical protein complex that consists of a proteolytic core and two regulatory complexes. These are responsible for recognition of ubiquitinated substrates, deubiquitination, and translocation to the core. Upon translocation, substrates are broken down into short peptide chains by caspase-like, trypsin-like, and chymotrypsin-like subunits (Jung, Catalgol & Grune 2009).

Regulation of C. elegans LIN-45 through ubiquitination

In addition to its activation cycle, LIN-45 activity in VPCs is also regulated by the ubiquitin-proteasome system. During the development of VPCs, levels of LIN-45 follow a specific pattern (Fig. 3). LIN-45 protein is present in all VPCs during the L2 stage. During L3, LIN-45 is degraded in P6.p. LIN-45 remains expressed in P5.p and P7.p throughout vulval formation (de la Cova et al., 2020). Because tertiary fate cells fuse with the large hypodermal cell, levels of LIN-45 become undetectable by fluorescence.

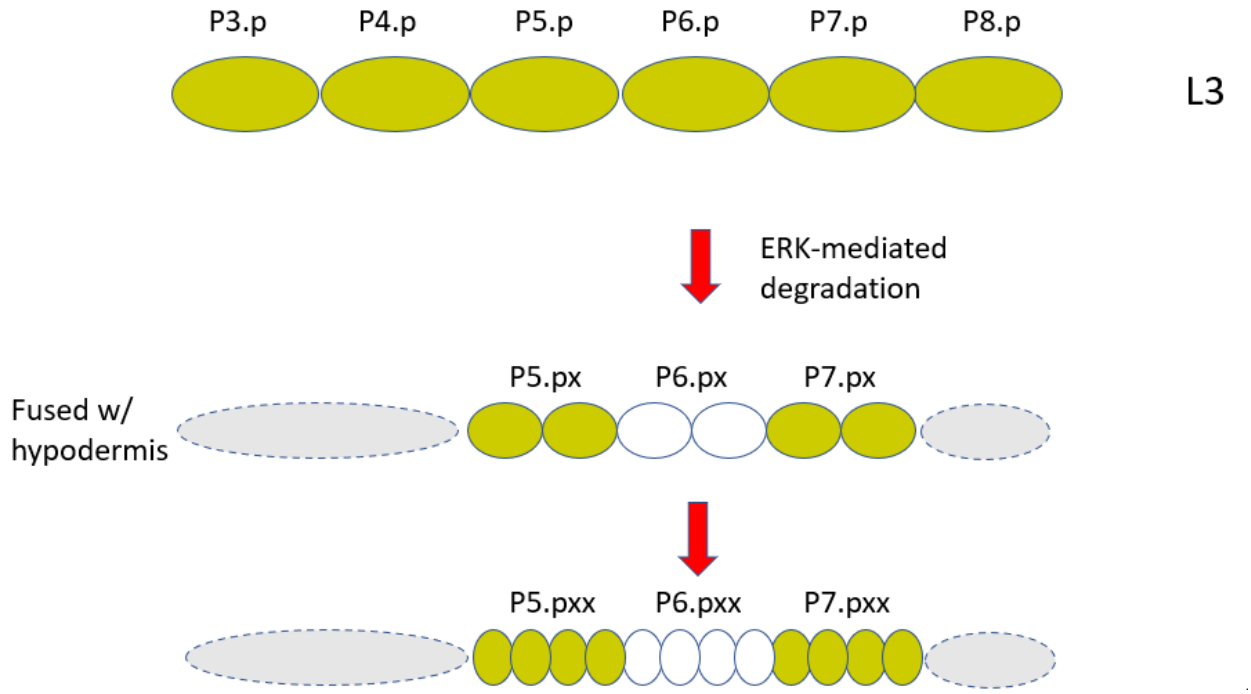

Figure 1.3. The developmental patterning of LIN-45 protein levels. LIN-45 is first expressed in all VPCs. During the L3 larval stage, LIN-45 is degraded in P6.p when SEL-10 recognizes the ERK-mediated phosphorylations of the CPD. Due to the lack of ERK activity in P5.p and P7.p, LIN-45 remains present in these VPCs. Once P3.p, P4.p, and P8.p fuse with the hypodermis, LIN-45 diffuses throughout the hypodermis and becomes undetectable by fluorescence.

SEL-10 is a conserved F-box protein and member of a multiprotein Skp1/Cul1/F-box (SCF) complex that acts as an E3 ubiquitin ligase. SEL-10 recognizes substrates for ubiquitination through physical interaction with a phosphorylated degron called the Cdc4 phosphodegron (CPD) (Welcker & Clurman 2008). Loss of function mutations in SEL-10 lead to LIN-45 accumulation in P6.p (de la Cova & Greenwald, 2012). LIN-45 contains a CPD sequence with a high degree of similarity to other SEL-10 substrates, and mutations in the CPD also lead to accumulation of LIN-45 in P6.p. In humans, the SEL-10 ortholog FBXW7 is required for ubiquitination of BRAF (Yeh et al. 2020).

It is possible that CPD phosphorylation is performed by the kinases GSK-3, CDK-2, and MPK-1, because loss of any of these kinases results in increased LIN-45 levels in P6.p

(de la Cova et al., 2020). It is interesting that the downstream kinase MPK-1 regulates LIN-45 degradation, as this suggests the presence of a negative feedback loop (de la Cova & Greenwald 2012). This negative feedback loop also exists in humans, as ERK phosphorylates BRAF at several sites, inhibiting its ability to bind to activated Ras (Ritt et al. 2020).

The UFD-2 protein network

UBE4B/UFD-2 is an E3/E4 ubiquitin ligase (Hoppe et al., 1999) that has been found to have roles in regulating ubiquitin-mediated degradation of substrates. In *C. elegans*, much of our understanding of UFD-2 enzymatic activity comes from studies of its ability to ubiquitinate UNC-45 (Hoppe et al., 2004, Hellerschmied et al., 2018). For example, UFD-2 can act as an E3 to ubiquitinate UNC-45 by itself, but it assembles much longer chains when its activity is combined with that of its partner E3 ubiquitin ligase CHIP/CHN-1, thus acting as an E4. UFD-2 was found to selectively ubiquitinate UNC-45 *in vitro* by binding to its tetratricopeptide repeat (TPR) domain, using the nearby UCS domain for stabilization of complex formation. The TPR domain of CHN-1 is required for binding to UFD-2 (Hoppe et al., 2004), indicating that UFD-2 may specifically target its interacting partners through binding to their TPR domains.

Another protein of note that has been found to directly interact with UFD-2 is CDC48/p97/VCP (Richly et al., 2005). CDC48 is part of the AAA ATPase family of proteins and promotes degradation of ubiquitinated proteins. It acts as a segregase, exerting physical force to pull proteins out of complexes and thus facilitate their degradation by the proteasome (Baek et al., 2013). CDC48 has two structurally similar orthologs in *C. elegans*: CDC-48.1 and CDC-48.2 (Appendix B). CDC-48.1 has been

found to form a complex with UFD-2 and CHN-1 (Janiesch et al., 2007), and these three proteins were found to cooperate to regulate UNC-45 levels through ubiquitin-mediated degradation.

Summary of findings

We hypothesized that negative regulators of the Ras-Raf-MEK-ERK pathway act to inhibit signaling by the activating mutant LIN-45(V627E). In Chapter 2, we describe our findings that the E3/E4 ubiquitin ligase UFD-2 is a negative regulator of LIN-45 activity. We find that UFD-2 is required for LIN-45 protein degradation, and that it also regulates the activated LIN-45(V627E) form. We find that requirements for UFD-2-mediated LIN-45 degradation are different from the mechanisms that direct E3 ubiquitin ligase SEL-10-mediated degradation. We also find that the known UFD-2-interacting proteins CDC-48.1 and 2 are required for LIN-45 degradation.

CHAPTER 2 - THE E3/E4 UBIQUITIN LIGASE UFD-2 IS A NEGATIVE REGULATOR OF THE KINASE LIN-45

Abstract

Melanomas commonly carry a mutation, *BRAF(V600E)*, which activates the kinase BRAF, part of the Ras-Raf-MEK-ERK pathway. In *Caenorhabditis elegans,* the equivalent mutation, LIN-45(V627E), causes increased ERK activation and developmental defects. Here, we report the identification of the E3/E4 ubiquitin ligase UFD-2 as a negative regulator of LIN-45 activity. Loss of UFD-2 enhances ectopic vulval fate signaling phenotypes caused by LIN-45(V627E). We find that loss of UFD-2 causes increased endogenous LIN-45 protein accumulation in vulval precursor cells (VPCs). Using a VPC-specific LIN-45 reporter to quantify protein levels, we find that UFD-2 partially contributes to LIN-45 degradation and appears to act in the same pathway as the E3 ubiquitin ligase SEL-10. In contrast to SEL-10, we found that the Cdc4 phosphodegron (CPD) region of LIN-45 is not sufficient for regulation by UFD-2. Analysis of truncated LIN-45 protein reporters revealed that two regions of LIN-45 are required for regulation by UFD-2. A LIN-45 reporter with mutations at both conserved 14-3-3 binding sites is regulated independently of UFD-2. We propose a model where 14-3-3 binding is required for UFD-2-dependent degradation of LIN-45. We also report that CDC-48.1/2, a known interactor of UFD-2, is required for degradation of LIN-45. These findings constitute identification of a previously unrecognized mechanism of LIN-45 regulation and indicate that further research is required to identify the requirements for this regulation.

Introduction

A significant portion of melanomas are derived from benign melanocytic nevi, where mutations in the genes *KRAS* and *BRAF* are frequently found, and a large proportion carry a single, activating mutation: *BRAF(V600E)*. Furthermore, melanoma growth requires activation of a kinase cascade downstream of Ras, involving the kinases BRAF, MEK1/2, and ERK1/2 (Lavoie and Therrien 2015) referred to throughout this work as Raf-MEK-ERK signaling. Although BRAF(V600E) exhibits constitutive kinase activity (Davies et al. 2002), detection of increased ERK kinase activity is relatively rare in the benign nevi samples where the *BRAF(V600E)* mutation is commonly found (Houben et al. 2008; Venesio et al. 2008). It is not completely understood what factors account for this discrepancy (Damsky and Bosenberg 2017). Furthermore, while melanoma growth can be suppressed by inhibition of Raf kinase activity, in clinical practice, development of drug resistance and disease relapse occurs frequently (Logue and Morrison 2012). These observations indicate that truly effective treatments for melanoma will require additional strategies.

In humans the proteins BRAF, RAF1, and ARAF are each Raf family members, while LIN-45 is the sole Raf ortholog in the nematode *Caenorhabditis elegans*. The functional domains and mechanisms of kinase activation are highly similar for each. Raf proteins consist of a N-terminal region with Ras-binding domain (RBD) and cysteine-rich domain (CRD), an intermediate “hinge” region, and a C-terminal kinase domain. When inactive, Raf is found in a monomeric, “closed” conformation characterized by an auto-inhibitory interaction between the N-terminal RBD-CRD domains and 14-3-3 proteins bound to the C-terminal region. Interaction with GTP-bound Ras via the RBD releases Raf from the

closed conformation and results in its recruitment to the plasma membrane. Further activation steps include Raf phosphorylation at several sites, culminating in dimerization and auto-phosphorylation within the kinase activation loop. In its fully activated state, the Raf kinase domain forms a dimer stabilized by dimerized 14-3-3 proteins bound to the C-terminal region.

Inactivation of Raf is also highly regulated, involving a variety of post-translational modifications. Within minutes of Raf-MEK-ERK pathway stimulation, Raf is phosphorylated at several sites by the downstream kinase ERK, providing a mechanism of negative feedback (Dougherty et al. 2005; Ritt et al. 2010; Eisenhardt et al. 2016). ERK-directed phosphorylation within the Raf N-terminal region disrupts its interaction with Ras, while phosphorylation at the C-terminus disrupts Raf dimerization. Phosphorylation also occurs in a third cluster located in the hinge region, centered on a conserved motif termed a Cdc4-phosphodegron (CPD) and recognized by the highly conserved FBXW7/SEL-10, part of a multi-protein Skp/Cullin/Fbox E3 ubiquitin ligase. In *C. elegans*, the CPD and SEL-10 are both required for LIN-45 protein degradation stimulated by high ERK activity. This ERK-directed degradation appears to be conserved in human cells, where BRAF protein is poly-ubiquitinated and degraded in a FBXW7-dependent manner (Saei et al. 2018). Finally, completion of the Raf activation/inactivation cycle requires dephosphorylation by phosphatases including PP2A.

In this work, we use *C. elegans* expressing the constitutively active mutant *lin-45(V627E)* to model *BRAF(V600E)*. We discover that the highly conserved E3/E4 ubiquitin ligase UFD-2 acts to negatively regulate signaling by LIN-45(V627E). As

expected for a negative regulator, loss of *ufd-2* enhances phenotypes resulting from the hyperactive *lin-45(V627E)* and suppresses phenotypes caused by partial loss-of-function alleles of *lin-45*. We show that *ufd-2* loss increases the degree of ERK activation and ectopic cell fate specification in *lin-45(V627E)*-expressing vulval precursor cells (VPCs) during larval development. We generated fluorescently-tagged endogenous and transgene reporters of LIN-45 protein in VPCs, and find that UFD-2 is required for LIN-45 protein degradation in VPCs where ERK activation is high, and that it likely acts by promoting the SEL-10-mediated degradation previously described. However, surprisingly, UFD-2 differs from SEL-10 in its substrate requirements within LIN-45. While solely the phosphorylated CPD is necessary for regulation by SEL-10, we find that regulation by UFD-2 requires multiple domains of LIN-45, and specifically that both conserved 14-3-3-binding sites are critical. We also investigated the roles of potential UFD-2-interacting proteins, finding that the chaperone-related AAA ATPases CDC-48.1 and CDC-48.2 are required for LIN-45 protein degradation. As the network of UFD-2 and CDC-48 proteins are highly conserved, these findings may lead to new insights in the regulation of human Raf proteins.

Results

UFD-2 is a negative regulator of LIN-45

To understand cellular mechanisms that modulate signaling by the mutant BRAF(V600E), we generated *C. elegans* transgenic strains carrying integrated, single-copy transgenes expressing the same mutation in the worm Raf ortholog, *lin-45(V627E)* (Fig. S1A). A small proportion of adult hermaphrodites carrying *lin-45(V627E)* transgenes display a Multivulva (Muv) phenotype (de la Cova, et al. 2020) characteristic of hyperactive Raf-MEK-ERK signaling; however, the majority are wild-type in appearance (Fig. 1A). In a forward genetic screen, we isolated a recessive mutant that displays a strongly penetrant Muv phenotype in combination with *lin-45(V627E)*; this strain carries a nonsense mutation in *ufd-2* (Fig. S1B,C). To confirm the role of *ufd-2*, we examined the phenotype of mutants carrying the null allele *ufd-2(tm1380)* (Hoppe et al. 2004), which we refer to as *ufd-2(0)* throughout this work. Although *ufd-2(0)* mutants never display a Muv phenotype in the presence of *lin-45(+)*, mutants carrying a *lin-45(V627E)* transgene display a Muv phenotype characterized by several ectopic pseudovulvae (Fig. 1A).

For analysis of *ufd-2* function, we examined *covTi106*, a *lin-45(V627E)* transgene that causes a Muv phenotype in approximately 14% of adult hermaphrodites (Fig. 1B). In *ufd-2(0)* mutants, the frequency of Muv phenotype is significantly enhanced, affecting 76% of adults. The Muv phenotype is reverted by the introduction of a single-copy transgene expressing wild-type *ufd-2(+)* specifically in VPCs (Fig. 1B), confirming that UFD-2 acts to prevent the Muv phenotype resulting from *lin-45(V627E).* Furthermore, the requirement for UFD-2 activity is likely cell-autonomous to VPCs.

UFD-2 is the sole *C. elegans* ortholog of human UBE4B, a U-box protein thought to have E3 and E4 ubiquitin ligase activities and to catalyze the poly-ubiquitin chain formation that target substrates for proteasome-mediated degradation (Hatakeyama and Nakayama 2003; Hellerschmied et al. 2018). Our discovery of UFD-2 as a factor that represses the Muv phenotype resulting from *lin-45(V627E)* prompted us to investigate how its role relates to another E3 ubiquitin ligase, SEL-10. We previously showed that SEL-10 promotes LIN-45 protein degradation and that its recognition of LIN-45 is mediated by a conserved Cdc4-phosphodegron (CPD) (de la Cova and Greenwald 2012). As previously reported, the Muv phenotype resulting from *lin-45(V627E)* was significantly enhanced in the null mutant *sel-10(ok1632)*, referred to throughout as *sel-10(0)* (Fig. 1B). To determine whether UFD-2 and SEL-10 act in the same or parallel pathways to influence the Muv phenotype, we examined the phenotype of *ufd-2(0); sel-10(0)* double mutants. In animals lacking both *ufd-2* and *sel-10*, the penetrance and expressivity of the Muv phenotype was significantly increased compared to either single mutant (Fig. 1B). The additive effect observed suggests that UFD-2 and SEL-10 act in parallel processes.

If UFD-2 regulates LIN-45 activity, then loss of *ufd-2* may suppress phenotypes resulting from reduced LIN-45 activity. Two hypomorphic alleles of *lin-45* were examined; both alter the LIN-45 Ras-binding-domain (RBD) and result in partial loss of function and a partially-penetrant Rod-like larval lethal phenotype caused by failure to specify the duct cell during embryogenesis (Hsu et al. 2002; Abdus-Saboor et al. 2011) (Fig. 1C). We found that loss of *ufd-2* alone did not cause larval lethality. Compared to either *lin-45* hypomorphic mutant alone, the double *ufd-2(0); lin-45* mutant displayed a

moderate but highly significant reduction in larval lethality (Fig. 1C). These results are consistent with a role for UFD-2 in negatively regulating LIN-45 activity.

Loss of *ufd-2* enhances LIN-45(V627E) activity in VPCs

In the *C. elegans* hermaphrodite, formation of the vulva involves the patterning and cell fate specification of six epithelial blast cells named P3.p-P8, or vulval precursor cells (VPCs), reviewed in Shin and Reiner (2018) (Fig. 2A). During L2 and L3 larval stages, the anchor cell (AC) of the gonad produces LIN-3, an EGF-like inductive signal. Of the six VPCs, P6.p is located nearest to the AC, and responds to LIN-3 through activation of EGF receptor (EGFR) and Ras-Raf-MEK-ERK signal transduction. Activation of the *C. elegans* ERK ortholog MPK-1 occurs in L2 and L3 stages in P6.p. At the early L3 stage, MPK-1 activity results in a vulval cell fate termed primary and transcription of Delta/Serrate/LAG-2 (DSL) ligands. Expression of DSL ligands by P6.p constitutes a lateral signal, inducing Notch activation and a cell fate termed secondary in the neighboring P5.p and P7.p cells. MPK-1 and Notch signaling inhibit one another, resulting in a robust pattern of cell fate specification. VPCs which receive neither the inductive nor lateral signals adopt tertiary fate and fuse with the hypodermis syncytial cell hyp7.

Activated ERK directly phosphorylates LIN-1, ortholog of the transcriptional repressor Elk1, causing derepression of the DSL ligand *lag-2* specifically in P6.p (Zhang and Greenwald 2011). To assess the pattern of primary fate specification in VPCs, we used *arIs222,* a *lag-2* reporter transgene that drives expression of 2xNLS-tagRFP (Sallee and Greenwald 2015). Loss of *ufd-2* alone does not alter the P6.p-specific expression

pattern of the *lag-2* reporter (Fig. 2B). Expression of activated *lin-45(V627E)* in all VPCs causes ectopic *lag-2* reporter expression in a significant portion of larvae. However, *lag-2* expression by VPCs that are adjacent to one another is rare, consistent with previous observations (de la Cova and Greenwald 2012; de la Cova et al. 2020) and suggesting that LIN-45 signaling and the resulting MPK-1 activation is not strong enough to overcome lateral signaling by Notch. In larvae expressing *lin-45(V627E)*, loss of *ufd-2* enhances the frequency of ectopic *lag-2* reporter expression and the frequency of ectopic expression by adjacent VPCs (Fig. 2B). These results suggest that UFD-2 acts to reduce the level of MPK-1 activation by LIN-45(V627E) signaling.

We made use of ERK-KTR, an *in vivo* biosensor developed to monitor ERK activation (Regot et al. 2014) and adapted for *C. elegans* (de la Cova et al. 2017) to quantify the degree of MPK-1 activation in VPCs of *ufd-2* mutants. As a Kinase Translocation Reporter (KTR), ERK-KTR responds to MPK-1 activation through a change in its nucleo-cytoplasmic localization. In the presence of active MPK-1, the ERK-KTR protein is phosphorylated and localized to the cytoplasm. Conversely, in the absence of MPK-1, the ERK-KTR is not phosphorylated and accumulates in the nucleus. ERK-KTR localization can be expressed as a ratio of cytoplasmic to nuclear signal (Regot et al. 2014), where a higher Cyto/Nuc ratio indicates higher MPK-1 activation (Materials and Methods).

We examined a VPC-specific ERK-KTR reporter during the early L3 stage, a time when MPK-1 activation is robust in P6.p (de la Cova et al. 2017), and LIN-45 is subject to regulated protein degradation (de la Cova et al. 2020). In wild-type larvae, MPK-1 activation is significantly greater in P6.p than in all other VPCs (Fig. 2C). This restriction

of MPK-1 activity to P6.p was also observed in *ufd-2(0)* mutant larvae. MPK-1 activation in P6.p in *ufd-2(0)* mutants was moderately, but significantly elevated compared to that in P6.p in wild type, suggesting that UFD-2 normally dampens MPK-1 activity level. Expression of *lin-45(V627E)* does not affect P6.p but causes a significant increase in MPK-1 activation in P4.p, P5.p, P7.p, and P8.p. In *ufd-2(0)* mutants expressing *lin-45(V627E),* MPK-1 activation is significantly elevated above levels observed in +; *lin-45(V627E)* controls (Fig. 2C). MPK-1 activation in *ufd-2(0); lin-45(V627E)* larvae is particularly high in P4.p and P8.p cells, a pattern similar to the ectopic *lag-2* reporter expression we observed for this genotype (Fig. 2B). Together, the *lag-2* reporter and ERK-KTR results show that when combined with hyperactive *lin-45(V627E)*, loss of *ufd-2* function results in greater MPK-1 activation. It was more surprising that loss of *ufd-2* caused increased MPK-1 activation in P6.p in the presence of *lin-45(+)*. As P6.p is the only VPC affected, this finding suggests that UFD-2 regulates LIN-45 in cells where MPK-1 activity is high.

ufd-2 negatively regulates LIN-45 protein stability

UFD-2 has E3/E4 ubiquitin ligase enzymatic activities and a highly conserved role in promoting protein degradation. To test whether *ufd-2* loss impacts the degradation of endogenous LIN-45 protein, we generated N- and C-terminal GFP knock-in alleles of *lin-45* (Fig. S2A,B). To ensure that VPC patterning and cell fate specification was completed in the L3 stage larvae we scored, we examined the expression of endogenous, tagged LIN-45 protein in the descendants of divided VPCs (Materials and Methods). When tagged at either the C-terminus (Fig. 3A) or N-terminus (Fig. 3B), GFP-

tagged LIN-45 protein is visible in P5.p and P7.p. Endogenous LIN-45 protein is visibly lower in P6.p, an expression pattern consistent with previously described transgenic LIN-45 protein reporters (de la Cova and Greenwald 2012; de la Cova et al. 2020).

Loss of *ufd-2* increased the visible protein accumulation of GFP-LIN-45 in P6.p (Fig. 3B). Although partially penetrant, this increased accumulation is seen in 68% of *ufd-2(0)* larvae, a significantly higher portion than in wild type (Fig. 3C). Loss of *sel-10* also caused increased protein accumulation of GFP-LIN-45 in P6.p (Fig. S2C), and this increased accumulation is visible in 100% of *sel-10(0)* L3 larvae (Fig. 3C). These results indicate that UFD-2 contributes to LIN-45 protein degradation in P6.p. However, in contrast to SEL-10, UFD-2 is not absolutely required for this process.

Because loss of *ufd-2* causes intermediate and partially penetrant LIN-45 protein accumulation in P6.p, we also assessed the impact on a LIN-45 protein reporter better suited for quantitation. When YFP-tagged LIN-45 expression is driven using the VPC-specific *lin-31* promoter, protein accumulation is very low in P6.p, despite the activity of this promoter in six VPCs (de la Cova and Greenwald 2012). Loss of *ufd-2* significantly increases the visibility of YFP-LIN-45 in P6.p (Fig. 3D). To perform our quantitation, we measured YFP-LIN-45 levels in two contexts: P5.p, a cell where LIN-45 signaling is inactive, and P6.p, a cell where LIN-45 is activated. In *ufd-2(0)* mutants, the YFP-LIN-45 level in P5.p was unchanged; however, YFP-LIN-45 in P6.p was significantly increased compared to wild type (Fig. 3F). These results suggest that UFD-2 acts to promote LIN-45 degradation in cells where LIN-45 is activated.

Because loss of *sel-10* and *ufd-2* are additive in enhancing the Muv phenotype (Fig. 1B), we also tested whether this was true for LIN-45 protein levels. Loss of *sel-10*

caused a significant increase in level of the YFP-LIN-45 reporter in P6.p (Fig. 3F). However, *ufd-2(0); sel-10(0)* double mutants did not have greater YFP-LIN-45 levels compared to *sel-10(0)* mutants. This non-additive interaction is in contrast to our data on the Muv phenotype and suggests that with respect to LIN-45 protein levels, *sel-10* and *ufd-2* act in the same pathway.

We next tested whether *ufd-2* impacts levels of the mutant, activated LIN-45(V627E) protein. When expressed using the *lin-31* promoter, fluorescence intensity of mutant YFP-LIN-45(V627E) is significantly lower than YFP-LIN-45(+) (Fig. 3E). Similar to wild-type YFP-LIN-45(+), the YFP-LIN-45(V627E) mutant is degraded in P6.p, and loss of *ufd-2* significantly elevated the levels observed in P6.p (Fig. 3G). In contrast to YFP-LIN-45(+), loss of *ufd-2* also elevated levels of YFP-LIN-45(V627E) in P5.p. As our analysis of the ERK-KTR found that expression of *lin-45(V627E)* causes elevated MPK-1 activation, this observation in P5.p is consistent with a model whereby UFD-2 promotes LIN-45 degradation in any VPC where MPK-1 activity is high.

UFD-2-dependent degradation requires multiple domains of LIN-45

Our findings that UFD-2 and SEL-10 both promote LIN-45 protein degradation prompted us to compare the sequence requirements in LIN-45 protein for its regulation by each ubiquitin ligase. SEL-10 recognizes its substrates via an interaction with CPD motifs, reviewed in Yumimoto and Nakayama (2020). Indeed, a minimal CPD region of LIN-45 that is 64 amino acids in length is sufficient for SEL-10-dependent degradation in P6.p (de la Cova et al. 2020) (Fig. 4A). We tested whether degradation of the minimal CPD

region requires *ufd-2*. In contrast to full-length YFP-LIN-45, a YFP-tagged minimal CPD, YFP-LIN-45(418-480), is not significantly stabilized in *ufd-2(0)* mutants (Fig. 4B, C, compare to Fig. 3F). This observation suggests that full-length LIN-45 protein contains additional sequences, structural features, or protein-protein interactions outside of the CPD that are required for UFD-2-dependent regulation.

C. elegans LIN-45 contains several domains that are present in all three human Raf proteins (Fig. 4A). The N-terminal region of LIN-45 contains two functional domains: a Ras-binding domain (RBD) known to directly interact with GTP-bound Ras, and a cysteine-rich domain (CRD) found to have multiple functions. In an inactive Raf monomer, the CRD interacts with 14-3-3 proteins and stabilizes the auto-inhibited state. On the other hand, in an activated Raf complex, the CRD is thought to stabilize plasma membrane association via phospholipid binding. We tested the role of the N-terminus and RBD-CRD regions of LIN-45 by expressing a truncated form, YFP-LIN-45(288-813). In contrast to the full-length reporter, this form is degraded in both wild type and *ufd-2(0)* mutants (Fig. 4D), suggesting that a functional domain within this region confers regulation by UFD-2. We next tested the role of Ras-binding by the RBD region. Mutations in conserved residues Q95 and R118 have been shown to abolish Ras-binding *in vitro* (Block et al. 1996) and reduce LIN-45 function *in vivo* (Hsu et al. 2002). A mutant reporter containing these mutations, YFP-LIN-45(Q95A, R118A), is degraded in P6.p in wild type, but stabilized in *ufd-2(0)* mutants (Fig. 4D), suggesting that the protein interaction with Ras is not required for LIN-45 regulation by UFD-2.

We also tested the roles for LIN-45 sequences found at its C-terminus. The C-terminal region of LIN-45 contains a highly conserved kinase domain followed by a shorter C-

terminal “tail” also containing conserved sequences: a 14-3-3 binding site, several sites phosphorylated by ERK during negative feedback, and sequences that influence Raf dimerization (Ritt et al. 2010). A truncated reporter, YFP-LIN-45(1-747), lacks all sequence C-terminal to the kinase domain. In contrast to the full-length reporter, YFP-LIN-45(1-747) is degraded in wild type and *ufd-2(0)* mutants (Fig. 4E), suggesting that this region is needed for regulation by UFD-2. We also examined a longer form, YFP-LIN-45(1-772), that contains the 14-3-3 binding site but lacks the more C-terminal feedback phosphorylation sites. YFP-LIN-45(1-772) protein is degraded in wild type larvae but stabilized in *ufd-2(0)* mutants (Fig. 4E), indicating that its degradation is UFD-2-dependent. Because these two C-terminal truncations differ in the presence of a 14-3-3 binding site (Figs. 4A, 5A), we hypothesized that 14-3-3 binding is required for UFD-2-dependent degradation.

LIN-45 regulation by UFD-2 requires the presence of both 14-3-3 binding sites

Like human Raf proteins, LIN-45 contains two highly conserved 14-3-3 binding sites. Interaction of 14-3-3 proteins with Raf requires phosphorylation of serine residues. In LIN-45, the C-terminal 14-3-3 site is centered on S756, and a second 14-3-3 site located in the “hinge region” is centered on S312 (Fig. Figs. 4A, 5A). To understand the effect of 14-3-3 binding on UFD-2-dependent degradation, we examined alanine missense mutations at both S312 and S756 sites. In contrast to wild type YFP-LIN-45(+), the mutant protein YFP-LIN-45(S312A) accumulates visibly in P6.p (Fig. 5B). However, degradation of YFP-LIN-45(S312A) remains dependent on *ufd-2* (Fig. 5D). We next examined YFP-LIN-45(S312A, S756A), a mutant form lacking both 14-3-3

binding sites. Unlike YFP-LIN-45(+) or the single mutant YFP-LIN-45(S312A), this form was degraded robustly in both wild type and *ufd-2(0)* mutants, indicating that its degradation was independent of UFD-2. Taken together with our findings from the C-terminal truncations, these results suggest that degradation of LIN-45 by UFD-2 requires 14-3-3 binding.

An RNAi screen identifies CDC-48.1/2 as a negative regulator of LIN-45 stability

To identify other regulators of LIN-45 protein stability that act with UFD-2, we performed an RNAi screen of candidate genes, assessing the impact of their depletion on the level of YFP-LIN-45 in P6.p. The genes tested encode U-box proteins, E1, E2, E3, and E4 ubiquitin ligases, and proteins known to interact in a network including UFD-2, HSP70, and HSP90 family proteins. To perform this screen, we made use of the VPC-specific YFP-LIN-45 reporter and scored the presence or absence of YFP-LIN-45 in P6.p (Materials and Methods).

The chaperone-related AAA ATPase CDC-48/VCP is highly conserved in eukaryotes, and acts to segregate ubiquitinated protein substrates so that they are targeted to the proteasome (Richly et al. 2005). In *C. elegans*, the orthologs CDC-48.1 and CDC-48.2 were shown to associate with UFD-2 (Janiesch et al. 2007), suggesting they may work in a UFD-2 protein network. Our screen identified both *cdc-48.1* and *cdc-48.2* as genes required for protein degradation of YFP-LIN-45 in P6.p. Due to the similarity in their nucleotide sequence, it is likely that RNAi targeting of one gene also impacts the other. RNAi depletion of both genes, termed *cdc-48.1/2* RNAi, resulted in significantly increased level of YFP-LIN-45 in P6.p (Fig. 5E).

We reasoned that if CDC-48 proteins act with UFD-2, they may have the same substrate requirements that UFD-2 displays in its regulation of LIN-45. To investigate this possibility, we tested whether *cdc-48.1* and *cdc-48.2* are required for degradation of the minimal CPD region reporter YFP-LIN-45(417-480). As expected, *cdc-48.1/2* RNAi did not result in stabilization of the minimal CPD reporter (Fig. 5E). The *cdc-48.1/2* RNAi was capable of stabilizing full-length YFP-LIN-45(+), and *sel-10* RNAi stabilized YFP-LIN-45(417-480) (Fig. 5E), two positive results suggesting that the failure of *cdc-48.1/2* RNAi to impact YFP-LIN-45(417-480) degradation is not explained by ineffective gene knockdown. *cdc-48.1/2* appear to be dispensable for degradation of the minimal CPD, consistent with their possible role in UFD-2-mediated degradation. We next tested whether *cdc-48.1/2* RNAi impacts the mutant protein YFP-LIN-45(S312A, S756A), which lacks phosphorylation at 14-3-3 sites. Contrary to our expectations, *cdc-48.1/2* RNAi resulted in significantly elevated levels of mutant YFP-LIN-45(S312A, S756A) in P6.p (Fig. 5E). Taken together, these findings suggest that while UFD-2 may associate with CDC-48 proteins, the functions of UFD-2 and CDC-48 proteins in promoting LIN-45 degradation differ in their requirement for 14-3-3 binding.

Discussion

In this work, we identified the conserved E3/E4 ubiquitin ligase UFD-2 as a negative regulator of LIN-45 activity and protein stability. In this Discussion, we (i) propose a model that UFD-2 promotes LIN-45 protein degradation as part of MPK-1 and SEL-10-directed negative feedback, (ii) consider potential mechanisms by which UFD-2 may

recognize LIN-45 as a substrate, and (iii) consider how our findings offer new insights into mutations found in human Raf proteins.

Activity-regulated degradation of LIN-45

UFD-2 has a known role in protein quality control, regulating the ubiquitination of unfolded proteins. For example, an investigation of the best-characterized *C. elegans* UFD-2 substrate to date, the myosin chaperone UNC-45, determined that its regulation by UFD-2 was enhanced when UNC-45 is more unfolded (Hellerschmied et al. 2018). On the other hand, examination of endogenous UNC-45 revealed that its bulk protein levels and characteristic downregulation during muscle development were unaffected by loss of *ufd-2*. This role for UFD-2 in recognizing unfolded UNC-45 was associated with activity as a bona fide E3 ubiquitin ligase, sufficient for mono- and poly-ubiquitination of this substrate.

The observation that UFD-2 targets unfolded substrates does not completely account for our observations of LIN-45. For example, we found that endogenous LIN-45 protein accumulation was increased in *ufd-2* mutants. LIN-45 was not subject to UFD-2-dependent degradation in all VPCs. Rather, regulation by UFD-2 was observed in two contexts: i) in the presence of *lin-45(+)*, degradation occurred solely in P6.p, and ii) in animals expressing *lin-45(V627E)*, degradation occurred in other VPCs, such as P5.p. Interestingly, it did not appear that the activity state of LIN-45 itself confers regulation by UFD-2, because the strongly hyperactive mutant LIN-45(V627E), the moderately activated mutant LIN-45(S312A), and the inactive mutant LIN-45(Q95A, R118A) were all subject to UFD-2-dependent degradation in P6.p. We previously showed that the kinase MPK-1 and the E3 ubiquitin ligase SEL-10 participate in negative feedback

resulting in degradation of LIN-45 in P6.p (de la Cova et al. 2020). We propose that UFD-2 also plays a role in this feedback, promoting LIN-45 degradation specifically in cells with high MPK-1 activation. Our finding that *ufd-2* and *sel-10* loss are not additive with respect to LIN-45 protein levels also suggests that UFD-2 acts in the same process as SEL-10, further supporting this model.

UFD-2 substrate specificity

In contrast to SEL-10, for which a small CPD region is sufficient for substrate specificity, we found no single sequence or domain of LIN-45 was sufficient to confer regulation by UFD-2. The presence of multiple domains, including the N-terminal RBD-CRD region and the C-terminal 14-3-3 site, were required for UFD-2-dependent degradation. One possibility to explain this complex requirement is that UFD-2 is required for degradation when LIN-45 is integrated within a multi-protein quaternary structure. Indeed, cryo-electron microscopy studies have established that Raf can dimerize and Raf complexes are composed of a large network of proteins, including 14-3-3, KSR, and MEK (Kondo et al. 2019; Park et al. 2019).

We propose a model where LIN-45 present in multi-protein complex is partially protected from proteasome targeting; in this form, its efficient degradation requires the activities of UFD-2 and CDC-48 proteins. The enzymatic activity of CDC-48 as an ATP-dependent segregase suggest it may be capable of extracting LIN-45 protein from a complex quaternary structure, assisting in its proteasome targeting (Baek et al. 2013). On the other hand, yeast Ufd2p appears to play a role as an adaptor, bridging interactions between a ubiquitinated protein substrate and Cdc48p (Bohm et al. 2011). Given the close association of CDC-48 and UFD-2, it was surprising that *cdc-48.1* and

cdc-48.2 were required for the degradation of LIN-45(S312A, S756A), while *ufd-2* was not. However, in yeast, Ufd2p is not the sole adaptor for Cdc48p (Bohm et al. 2011). It is possible the ability of CDC-48 proteins to work with multiple adaptors may explain the difference in substrate requirements for UFD-2 and CDC-48.

In *C. elegans*, UFD-2 interacts with the substrate UNC-45 through a tetratricopeptide repeat (TPR) motif and a domain characterized by the proteins UNC-45/Cro1/She4p (UCS) (Hellerschmied et al. 2018). The TPR motif is a 34-amino acid motif found in repeats; a minimum of three are needed to form a helical structure frequently found in protein interaction domains (Das et al. 1998). While TPR motifs are not known to be present in Raf proteins, they may be unrecognized as this motif is highly degenerate. Alternatively, it is possible that another protein in Raf complexes contains TPR motifs. For example, HSP90 family members contain TPR sequences and are known to interact with Raf. Our findings suggest that 14-3-3 binding by LIN-45 is required for UFD-2-dependent degradation. In this light, it is intriguing that a structural (but not sequence) similarity has been found between TPR motifs and 14-3-3 proteins (Das et al. 1998).

New insights into mutations found in human Rafs

Our finds provide new insights into mutations that alter 14-3-3 binding sites in human Raf proteins. Although uncommon in human *BRAF*, mutations in human *RAF1* that alter the hinge region 14-3-3 site are observed in some cancers and in patients with Noonan and LEOPARD syndromes, diseases characterized by elevated Ras-Raf-MEK-ERK signaling. The mutant RAF1(S259A), which disrupts the serine normally phosphorylated at this site, causes increased phospho-MEK and phospho-ERK when introduced to

human cells (Pandit et al. 2007). By observing the analogous mutation in *C. elegans*, LIN-45(312A), we find this mutant protein is partially stabilized in P6.p compared to wild type LIN-45, suggesting it is partly resistant to negative feedback and degradation directed by MPK-1. Degradation is LIN-45(S312A) remains UFD-2-dependent, and the mechanism that accounts for its higher accumulation in P6.p is not yet known. To better understand whether a similar phenotype is seen in RAF1, it will be useful to investigate the protein degradation of RAF1 and RAF1(259A) in human cells.

Materials and Methods

C. elegans genetics

Strains used in this work are listed in Supplemental Information (Table S1). The following alleles were obtained from the Caenorhabditis Genetics Center (https://cgc.umn.edu/). LGII: *ufd-2(tm1380)*. LGIV: *lin-45(n2018), lin-45(n2506).* LGV: *sel-10(ok1632.* The RNAi-sensitized mutant *nre-1(hd20) lin-15B(hd126)* displays enhanced RNAi effectiveness in VPCs (Schmitz et al. 2007; Deng et al. 2019). The transgene *arIs222 [lag-2p::2xNLS-tagRFP::unc-54 3'UTR]* was previously described (Sallee and Greenwald 2015; Underwood et al. 2017). The transgene *arTi4 [lin-31p::YFP-lin-45(417-480)]* was previously described (de la Cova et al. 2020).

Plasmids and transgenes used for *lin-45* expression in *C. elegans*

Plasmids for *lin-45* reporter transgenes were generated following a method described in de la Cova and Greenwald (2012). Specifically, the YFP-coding sequence was fused in

frame with *lin-45* cDNA (Wormbase sequence Y73B6A.5a) to produce a sequence encoding N-terminally tagged YFP-LIN-45 protein. For expression of YFP-LIN-45 in VPCs, cDNAs were cloned into pCC395, an expression vector in a miniMos backbone (Frokjaer-Jensen et al. 2014) that contains a hybrid promoter derived from 5′ and intronic elements of the *lin-31* gene, designated *lin-31p* (Tan et al. 1998), and a 3′ UTR derived from the *unc-54* gene.

C. elegans alleles made by gene editing

The endogenous GFP knock-in alleles *cov37* and *cov40* (this work) were generated through CRISPR/Cas9 methods described in Dickinson et al. (2015); Dickinson and Goldstein (2016). All guide RNAs used in CRISPR/Cas9 editing were purchased from Integrated DNA Technologies. Plasmid repair templates containing a Hygromycin B-selectable self-excising cassette were introduced to produce insertions at either the start or stop codon of *lin-45*. Allele *cov37* contains an insertion at the start of *lin-45* isoform Y73B6A.5a, resulting in an N-terminal fusion encoding *GFP-3xFLAG-lin-45.* Allele *cov40* contains an insertion at the shared stop of all *lin-45* isoforms, resulting in a C-terminal fusion encoding *lin-45-3xFLAG-GFP*.

C. elegans reporters used to report or alter VPC gene expression

lin-45(V627E). The single-copy integrated transgenes *covTi106* and *covTi107* (this work) use the *lin-31p* elements to drive expression of a mutant cDNA, *lin-45(V627E)*, followed by the *unc-54* 3′ UTR.

VPC-specific ufd-2(+). The single-copy integrated transgene *covTi36* (this work) uses the *lin-31p* to drive expression of *ufd-2* cDNA (Wormbase sequence T05H10.5b), followed by the *unc-54* 3'UTR.

lag-2p::2xNLS-tagRFP. The integrated transgene *arIs222* (Sallee and Greenwald, 2015) uses 5′ sequences of the *lag-2* gene to drive expression of *2xNLS-tagRFP*. This reporter is expressed exclusively in P6.p and daughters at the L3 stage.

lin-31p::YFP-lin-45. The single-copy integrated transgene *covTi64* (this work) uses *lin-31p* to drive expression of a full-length YFP-tagged LIN-45 followed by the *unc-54* 3′ UTR.

***lin-31p::YFP-lin-45* mutant forms.** All mutant forms of *YFP-lin-45* use the same *lin-31p* and *unc-54* 3′ UTR to drive expression of the corresponding transgene. The transgenes include: *arTi4* [*yfp-lin-45(417-480)*], *covTi110* [*lin-31p::yfp-lin-45(288-813)*], *covTi158* [*lin-31p::yfp-lin-45(Q95A, R118A)*], *covTi54* [*lin-31p::yfp-lin-45(1-747)*], *covTi127* [*lin-31p::yfp-lin-45(1-772)*], *covTi101* [*lin-31p::yfp-lin-45(S312A)*], *covTi88* [*lin-31p::yfp-lin-45(S312A,S756A)*].

Assessment of Multivulva and L1 lethality phenotypes

To assess the Multivulva phenotype caused by *covTi106* [*lin-31p::lin-45(V627E)::unc-54 3'UTR*], L4 hermaphrodites from uncrowded cultures were picked to fresh plates; adults were examined ~24 h later using a dissecting microscope and scored for the presence of a normal vulva and the number of pseudovulvae. All *lin-45(+)* and *lin-45(V627E)* animals scored for the Multivulva phenotype were grown at 20°C.

To assess L1 lethality of *lin-45* hypomorphic mutants, L4 hermaphrodites were picked individually and transferred to fresh plates daily. At ~48 h after egg laying, progeny were examined at the dissecting microscope and scored as live larvae, dead larvae, or unhatched eggs.

Qualitative scoring of *lag-2* reporter expression in VPCs

To score lag-2 reporter expression in the L3 larval stage, 12-16 hour egg collections were performed and grown at 20°C. At ~2 days after egg collection, live larvae were mounted on an agarose pad in M9 buffer containing 10 mM levamisole and examined using a Zeiss Axio Imager microscope. To further refine the developmental stage of larvae scored, only L3 larvae in which it was evident that VPCs had undergone either one or two cell divisions were scored. Location of VPC descendants was determined using DIC optics, and expression of the RFP transgene *arIs222* [*lag-2p::2xNLS-tagRFP*] was scored on a positive/negative basis. VPC daughters of P3.p, P4.p, and P8.p which had fused with the hypodermis were scored as negative.

RNAi treatment in *C. elegans*

Each bacteria strain was grown in liquid culture and spread on NGM plates containing IPTG inducer, as previously described (Kamath and Ahringer 2003). All strains assayed carried the mutations *nre-1(hd20) lin-15B(hd126), and* were synchronized by a standard bleach/sodium hydroxide protocol to prepare eggs (Stiernagle 2006). Approximately 200 eggs were placed on each RNAi-feeding plate and grown at 20°C. L3 stage larvae were

examined after ~44 h, a time point when larvae of early, mid and late L3 stage were easily found. Larvae were anesthetized in M9 buffer containing 10 mM levamisole, and the presence of YFP fluorescence in VPC daughter cells or granddaughter cells was scored quantitatively as described below.

Imaging of *C. elegans*

For all imaging, live larvae were mounted on an agarose pad in M9 buffer containing 10 mM levamisole. Images used for quantitation were acquired using a Nikon Ti inverted microscope equipped with a spinning disk confocal system (Crest Optics) and dual sCMOS cameras (Teledyne Photometrics).

To assess ERK-KTR localization in VPCs at the early L3 larval stage, animals were synchronized using 2-hour egg collections, grown at 25°C, and imaged at ~28 hours after egg collection. Z-stacks of mClover and mCherry were acquired simultaneously at 60x; for all images, exposure time and laser power used for mClover and mCherry were equal: 500 ms and 25% laser power. For all ERK-KTR experiments, blank images were acquired using the same parameters.

To quantify YFP-tagged LIN-45 reporter expression in L3 larvae, 12-16 hour egg collections were performed, grown at 20°C, and imaged at ~2 days after egg collection. To further refine the developmental stage of larvae scored, only L3 larvae in which it was evident that VPCs had undergone either one or two cell divisions were scored. Z-stacks of YFP were acquired using a 40x objective and the microscope and spinning

disk system described above; for all images, an exposure time of 500 ms and laser power of 25% was used.

Image quantitation and analysis

The subcellular localization of the ERK-KTR biosensor was quantified using methods described in de la Cova, et al. (2017) and the Nikon NIS-Elements software. Briefly, illumination correction and background subtraction was performed using the blank images obtained during each experiment. Image segmentation followed by manual curation was performed in NIS-Elements to create regions of interest (ROIs) for the nucleus and cytoplasm of VPCs P4.p, P5.p, P6.p, P7.p, and P8.p. (P3.p fuses with the hyp7 syncytium in approximately half of animals and was not analyzed.) Mean fluorescence intensity for mClover within the nucleus and cytoplasm was determined for up to five of the most equatorial Z slices per cell. Data presented is a ratio of the mean cytoplasmic mClover intensity/mean nuclear mClover intensity, referred to as "Cyto/Nuc" ratio, per individual cell.

The expression of YFP-tagged LIN-45 protein was quantified using NIS-Elements software. ROIs for the cytoplasm of daughters or grand-daughters of P5.p, P6.p, and P7.p were created manually in NIS-Elements. While all other YFP-LIN-45 reporters were exclusively cytoplasmic, the truncated YFP-LIN-45(417-480) form was both cytoplasmic and nuclear. For this reason, the nucleus was included in the quantification of this mutant. Data presented is the mean YFP fluorescence intensity for the most equatorial Z slice, per set P5.p or P6.p descendants.

Statistical analysis

For the Muv, L1 lethal, and ectopic *lag-2* expression phenotypes, we compared the frequency of a phenotype in two groups using the Fisher's exact test to calculate a two-tailed *P*-value. For quantitative measurements of ERK-KTR Cyto/Nuc ratio and YFP reporter fluorescence intensity, we compared the means of multiple groups by performing a one-way ANOVA followed by multiple pairwise comparisons and Bonferroni correction to calculate a two-tailed *P*-value. All statistical analyses were performed using GraphPad Prism software.

Figures

Figure 2.1

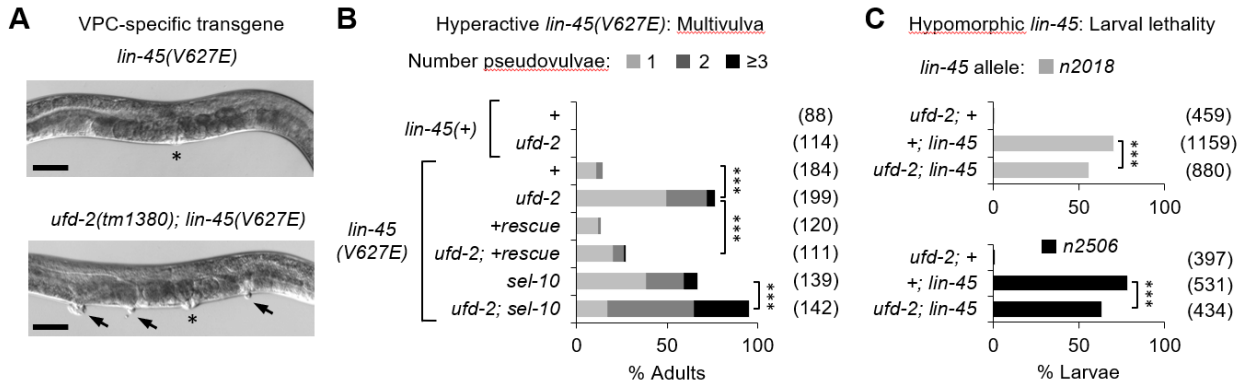

Figure 2.1. UFD-2 is a negative regulator of LIN-45 function. A) Top; an adult hermaphrodite carrying covTi106 expresses the hyperactive lin-45(V627E). Bottom; covTi106 causes a highly penetrant Multivulva phenotype in the null mutant ufd-2(tm1380). Animals are shown with anterior at left, dorsal at top. Asterisk indicates location of the vulva; arrowheads indicate locations of pseudovulvae. Scale bar, 50 µm. B) Pseudovulvae displayed by adult hermaphrodites shown as percentage of adults with 1, 2, 3 or greater numbers of pseudovulvae. lin-45(+) control genotypes were wild-type for ufd-2 (+) or null (tm1380). Genotypes carrying the lin-45(V627E) transgene covTi106 included: ufd-2(+), ufd-2(tm1380), the ufd-2 rescue transgene covTi36 [lin-31p::ufd-2(+)] alone or with ufd-2(tm1380), the sel-10(ok1632) mutant alone or with ufd-2(tm1380). The number of adults scored (n) is indicated in parentheses. A Fisher's exact test was used to compare the number of Multivulva adults. *** indicates the p-value <0.0001. C) Rod-like lethality at the L1 larval stage displayed by mutants lin-45(n2018) and lin-45(n2506), shown as percentage of larvae. Genotypes scored were either ufd-2(tm1380), or lin-45 hypomorphs, or ufd-2; lin-45 double mutants. All genotypes for the lin-45(n2018) experiment carried the mutation dpy-20(e1282), while all genotypes for the lin-45(n2506) experiment carried the mutation unc-24(e138). The number of larvae scored (n) is indicated in parentheses. A Fisher's exact test was used to compare the number of Rod-like larvae. *** indicates the p-value <0.0001. Complete strain genotypes for B) and C) are in Supplemental Table S1.

Figure 2.2

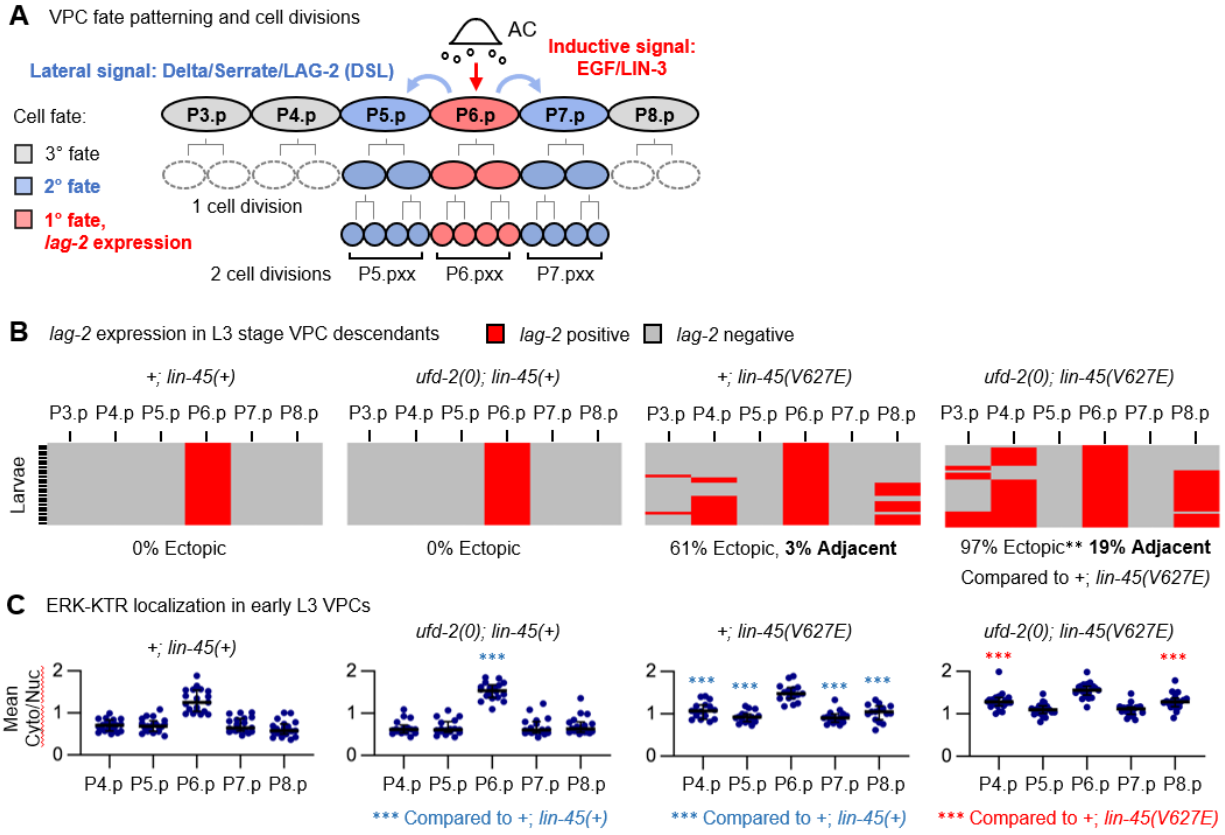

Figure 2.2 UFD-2 negatively regulates LIN-45 in VPCs. A) VPC fate patterning and cell divisions. In the L2 larval stage, an inductive signal produced by the anchor cell (AC) activates EGFR and Ras-Raf-MEK-ERK signaling in P6.p. During the L3 stage, P6.p expresses the LAG-2 lateral signal, activating Notch/LIN-12 in P5.p and P7.p. B) VPC fates, assessed using the 1° fate reporter *arIs222[lag-2p::2xNLS-tagrfp]*. In all panels, rows represent individual larvae, and columns represent different VPCs. Red, *lag-2* is expressed; gray, *lag-2* is not expressed. The percentage displaying ectopic *lag-2* expression (% Ectopic), or expression in adjacent VPCs (% Adjacent) is indicated. Genotypes with *lin-45(+)* are in wild type (n=37) or *ufd-2(0)* mutants (n=36). The transgene *covTi107* was used to express LIN-45(V627E) in wild type (n=31) or *ufd-2(0)* mutants (n=36). The Fisher's Exact Test was performed to compare the number of larvae with ectopic 1º fate, and the relevant comparison is indicated. C) MPK-1 activation in individual VPCs was assessed using ERK-KTR localization, where a higher Cyto/Nuc ratio corresponds to higher MPK-1 activation. Data points represent the mean Cyto/Nuc for individual VPCs. Genotypes with *lin-45(+)* are in wild type (n=19) or *ufd-2(0)* mutants (n=18). *covTi107* genotypes expressing LIN-45(V627E) are in wild type (n=15) or *ufd-2(0)* mutants (n=19). To test for significant differences in Cyto/Nuc ratio, a one-way ANOVA was performed, followed by multiple comparisons and Bonferroni correction. ***p-value <0.0001; **p-value <0.001.

Figure 2.3

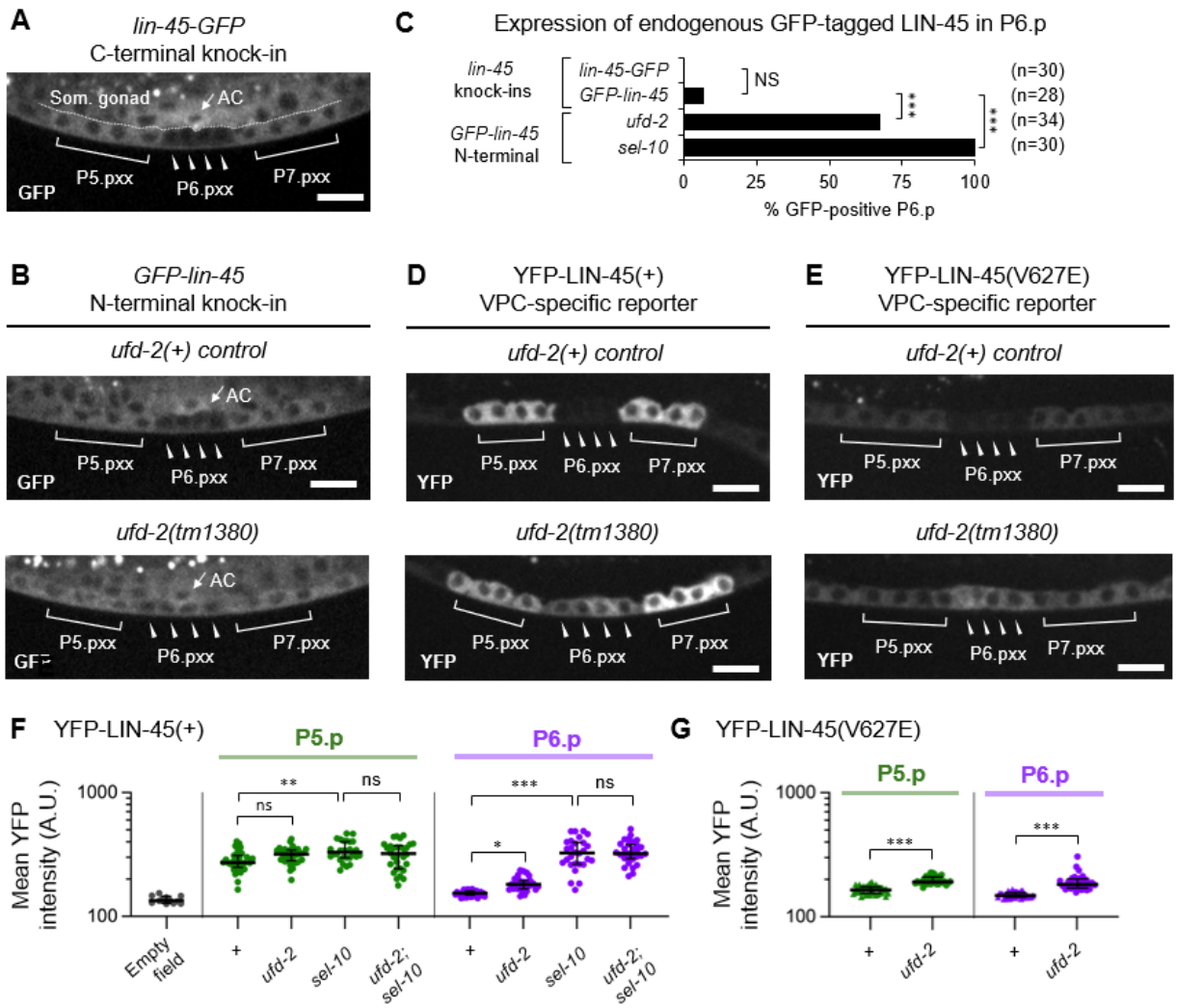

Figure 2.3. UFD-2 is required for LIN-45 protein degradation. In all panels, cells produced by VPCs are shown at the L3 larval stage; descendants of P5.p, P6.p, and P7.p are labeled P5.pxx, P6.pxx, and P7.pxx, respectively. A) Endogenous LIN-45-GFP, tagged at the C-terminus. B) Endogenous GFP-LIN-45, tagged at the N-terminus. Shown are wild type (top) and *ufd-2(0)* mutant (bottom). C) The percentage of larvae that displayed high levels of endogenous tagged LIN-45 in P6.p descendants, in wild type and *ufd-2(0)* and *sel-10(0)* mutants. The number of larvae scored (n) is indicated. D) The transgenic reporter YFP-LIN-45(+) in wild type (top) and *ufd-2(0)* mutants (bottom). E) The mutant YFP-LIN-45(V627E) in wild type (top) and *ufd-2(0)* mutants (bottom). F-G) Expression of YFP-tagged LIN-45 reporters in P5.p (green) and P6.p (purple). To display data from bright and dim cells together, the mean YFP intensities are plotted on a $\log_{10}$ scale. F) YFP-LIN-45(+) levels in wild type (n=32), *ufd-2(0)* (n=33), *sel-10(0)* (n=28), and *ufd-2(0); sel-10(0)* (n=30). G) YFP-LIN-45(V627E) levels in wild type (n=36) and *ufd-2(0)* (n=32). To test for significant differences in YFP intensity, a one-way ANOVA was performed, followed by multiple comparisons and Bonferroni correction. *p-value <0.01. ***p-value <0.0001.

Figure 2.4

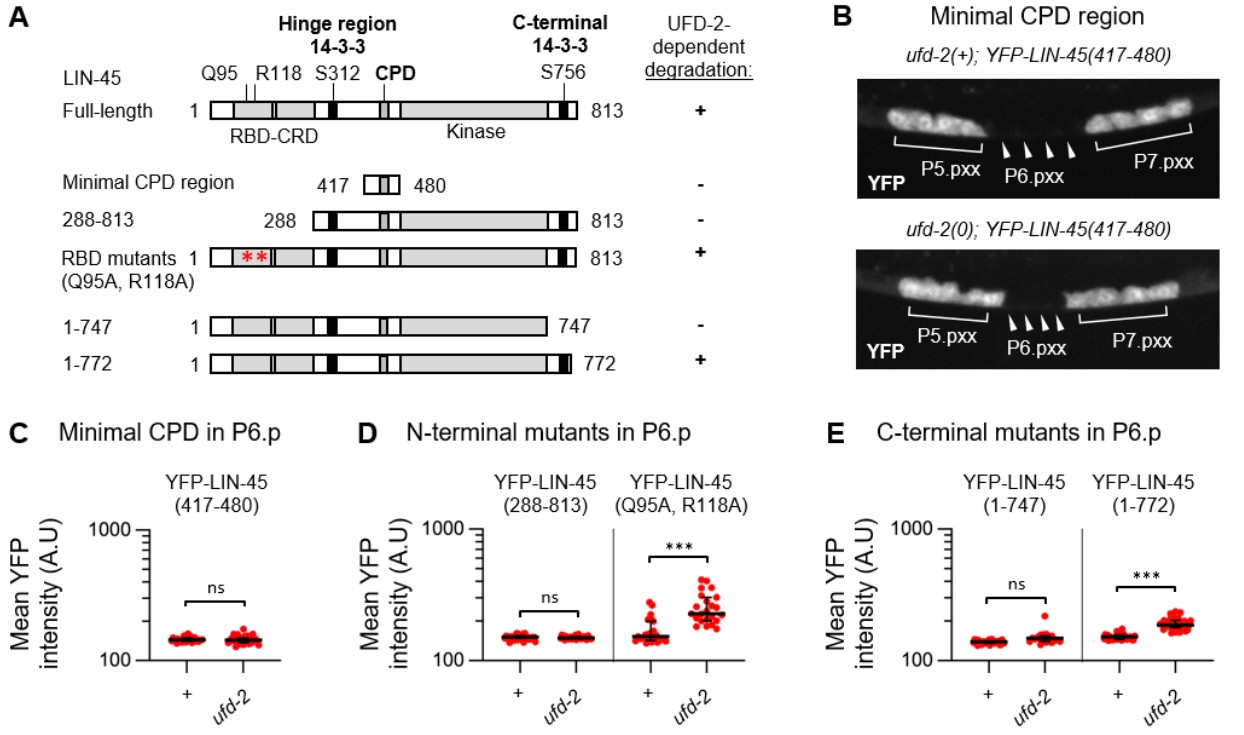

Figure 2.4. UFD-2-dependent degradation requires multiple domains of LIN-45. A) The functional domains of LIN-45 include the Ras-binding domain (RBD), cysteine-rich domain (CRD), hinge region 14-3-3 site, Cdc4-phosphodegron (CPD), kinase domain, and C-terminal 14-3-3 site. Wild-type and mutant forms of YFP-tagged LIN-45 were examined in *ufd-2(0)* mutants to determine whether their degradation was UFD-2 dependent (indicated by +) or independent (indicated by -). B) The YFP-LIN-45(417-480) reporter contains a minimal CPD region. Shown are YFP-LIN-45(417-480) in wild type (top) and *ufd-2(0)* mutants (bottom). The descendants of P5.p, P6.p, P7.p are labeled P5.pxx, P6.pxx, and P7.pxx respectively. C-E) Expression of YFP-tagged LIN-45 reporters in P6.p. The mean YFP intensity in P6.p is plotted on a $\log_{10}$ scale. C) The truncated YFP-LIN-45(417-480) in wild type (n=31) and *ufd-2(0)* (n=31). D) The N-terminal truncated form YFP-LIN-45(288-813) in wild type (n=36) and *ufd-2(0)* (n=32). A mutant deficient in Ras-binding, YFP-LIN-45(Q95A, R118A), in wild type (n=23) and *ufd-2(0)* (n=23). E) The C-terminal truncated form YFP-LIN-45(1-747), in wild type (n=31) and *ufd-2(0)* (n=19). A truncation that includes the C-terminal 14-3-3 site, YFP-LIN-45(1-772), in wild type (n=35) and *ufd-2(0)* (n=36). To test for significant differences in YFP intensity, a one-way ANOVA was performed, followed by multiple comparisons and Bonferroni correction. ***p-value <0.0001.

Figure 2.5

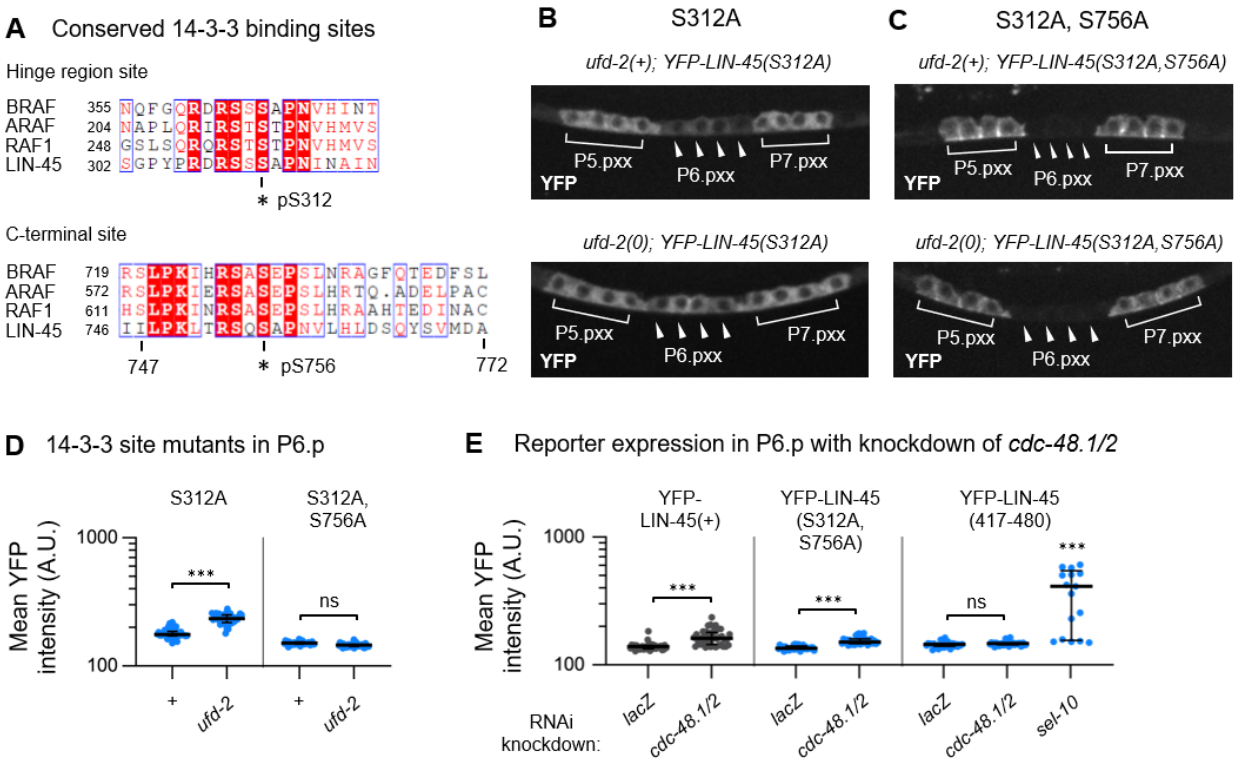

Figure 2.5. UFD-2-dependent degradation requires the 14-3-3 binding sites of LIN-45. A) Alignments of protein sequence from 14-3-3 binding sites found in the hinge region (top) and C-terminus (bottom) of human BRAF, ARAF, CRAF, and *C. elegans* LIN-45. Indicated are the sites of phosphorylation (asterisks), and endpoints of C-terminal truncated YFP-LIN-45 reporters. B-C) In all panels, cells produced by VPCs are shown at the L3 larval stage; descendants of P5.p, P6.p, and P7.p are labeled P5.pxx, P6.pxx, and P7.pxx, respectively. B) The mutant YFP-LIN-45(S312A) reporter in wild type (top) and *ufd-2(0)* mutants (bottom). C) The mutant YFP-LIN-45(S312A, S756A) reporter in wild type (top) and *ufd-2(0)* mutants (bottom). D) Expression of YFP-tagged LIN-45 reporters in P6.p. The mean YFP intensity in P6.p is plotted on a $\log_{10}$ scale. Shown are YFP-LIN45(S312A) in wild type (n=42) and *ufd-2(0)* (n=39), and YFP-LIN-45(S312A, S756A) in wild type (n=33) and *ufd-2(0)* (n=33). E) Expression of YFP-tagged LIN-45 reporters in P6.p of RNAi-treated L3 stage larvae (Materials and Methods). The mean YFP intensity in P6.p is plotted on a $\log_{10}$ scale. RNAi-mediated knockdown was used to deplete the genes *cdc-48.1* and *cdc-48.2* simultaneously. Shown are the full-length YFP-LIN-45(+) reporter in the negative control *lacZ* RNAi (n=33) and *cdc-48.1/2* RNAi (n=42), the mutant YFP-LIN-45(S312A, S756A) reporter in *lacZ* RNAi (n=32) and *cdc-48.1/2* RNAi (n=29), and the truncated minimal CPD YFP-LIN-45(417-480) reporter in *lacZ* RNAi (n=31), *cdc-48.1/2* RNAi (n=36), and *sel-10* RNAi (n=17). To test for significant differences in YFP intensity, a one-way ANOVA was performed, followed by multiple comparisons and Bonferroni correction. ***p-value <0.0001.

Supplemental Information

Table S1: *C. elegans* strains used in this work

Strain	Genotype	Figure
N2	wild type isolate	1
PP198	ufd-2(tm1380)	1
MKE339	covTi106 [lin-31p::lin-45(V627E)::unc-54 3'UTR]	1
MKE341	ufd-2(tm1380); covTi106	1
MKE128	covTi36 [lin-31p::ufd-2::unc-54 3'UTR]	1
MKE372	covTi36; covTi106	1
MKE343	covTi106; sel-10(ok1632)	1
MKE392	ufd-2(tm1380); covTi106; sel-10(ok1632)	1
MKE236	ufd-2(tm1380); dpy-20(e1282)	1
WU48	lin-45(n2018) dpy-20(e1282)	1
MKE237	ufd-2(tm1380); lin-45(n2018) dpy-20(e1282)	1
MKE242	ufd-2(tm1380); unc-24(e138)	1
WU49	lin-45(n2506) unc-24(e138)	1
MKE241	ufd-2(tm1380); lin-45(n2506) unc-24(e138)	1
GS7090	arIs222 [lag-2p::2xNLS-tagRFP]	2
MKE111	ufd-2(tm1380); arIs222	2
MKE363	covTi107 [lin-31p::lin-45(V627E)::unc-54 3'UTR]; arIs222	2
MKE365	ufd-2(tm1380); covTi107; arIs222	2
MKE246	covTi15 [lin-31p::ERK-KTR-mClover-T2A-mCherry-his-58::unc-54 3'UTR]	2
MKE248	ufd-2(tm1380); covTi15	2
MKE387	covTi15; covTi107	2
MKE388	ufd-2(tm1380); covTi15; covTi107	2

MKE277	lin-45(cov40)	3
MKE243	lin-45(cov37)	3
MKE267	ufd-2(tm1380); cov37	3
MKE291	cov37; sel-10(ok1632)	3
MKE232	covTi64 [lin-31p::yfp-lin-45::unc-54 3'UTR]	3
MKE234	ufd-2(tm1380); covTi64	3
MKE266	covTi64; sel-10(ok1632)	3
MKE440	ufd-2(tm1380); covTi64; sel-10(ok1632)	3
MKE441	covTi126 [lin31p::yfp-lin-45(V627E)]	3
MKE442	ufd-2(tm1380); covTi126	3
GS7738	arTi4 [lin-31p::yfp-lin-45(417-480)::unc-54 3'UTR]	4
MKE142	ufd-2(tm1380); arTi4	4
MKE382	covTi110 [lin-31p::yfp-lin-45(417-480)::unc-54 3'UTR]	4
MKE384	ufd-2(tm1380); covTi110	4
MKE436	covTi158 [lin-31p::yfp-lin-45(Q95A,R119A)::unc-54 3'UTR]	4
MKE437	ufd-2(tm1380); covTi158	4
MKE181	covTi54 [lin-31p::yfp-lin-45(1-747)::unc-54 3'UTR]	4
MKE192	ufd-2(tm1380); covTi54	4
MKE426	covTi127[lin-31p::yfp-lin-45(1-772)::unc-54 3'UTR]	4
MKE427	ufd-2(tm1380); covTi127	4
MKE310	covTi101 [lin-31p::yfp-lin-45(S312A)::unc-54 3'UTR]	5
MKE312	ufd-2(tm1380); covTi101	5
MKE273	covTi88 [lin-31p::yfp-lin-45(S312A,S756A)::unc-54 3'UTR]	5
MKE335	ufd-2(tm1380); covTi88	5
MKE422	covTi64; nre-1(hd20) lin-15B(hd126)	5
MKE423	covTi88; nre-1(hd20) lin-15B(hd126)	5
GS7825	arTi4; nre-1(hd20) lin-15B(hd126)	5

Table S2: Gene-specific guide RNAs used for CRISPR/Cas9-mediated gene editing

All gene-editing strategies made use of the universal Alt-R-Crispr-Cas9 tracrRNA (Integrated DNA Technologies catalog #1072532), plus a custom gene-specific Alt-R crRNA targeting the following DNA sequences:

Guide name	**20-nucleotide DNA sequence targeted**	**For allele**
Ce.Cas9.LIN-45.1.AJ	5’- TGAAATTAATCCGACTCATT -3’	*cov37*
crMKE2	5’- AAGGCATACTACAATGTCTA -3’	*cov40*

Supplemental Figure S1

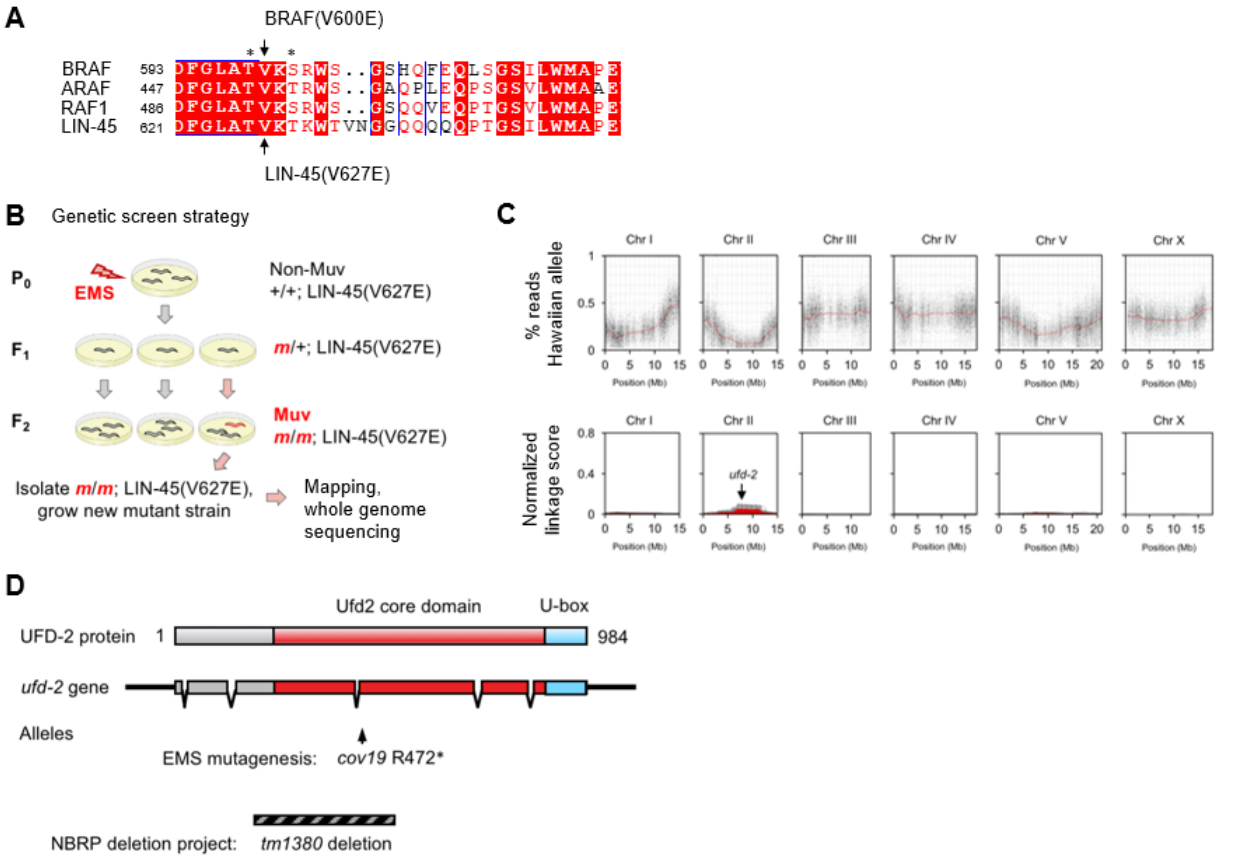

Figure 2.S1. The *lin-45(V627E)* mutation and identification of a novel *ufd-2* mutant. A) Alignment of protein sequence in the kinase activation loop of human Raf proteins BRAF, ARAF, RAF1, and *C. elegans* LIN-45. Indicated are the residues phosphorylated in wild-type Raf proteins (asterisks), and the valine residue mutated in BRAF(V600E) and LIN-45(V627E) (arrows). B) Diagram of EMS mutagenesis screen for for mutations that enhance the Multivulva (Muv) phenotype resulting from *lin-45(V627E).* C) Linkage data used to map the chromosome location of the recessive mutation *cov19*. A mutant strain carrying *lin-45(V627E)* and *cov19* was outcrossed to the Hawaiian wild-type isolate CB4856. Genomic DNA was pooled from the progeny of at least 50 F2 hermaphrodites displaying a severe Muv phenotype, presumptive *cov19* homozygotes. Reads from whole genome sequencing were analyzed to determine the percentage composition by Hawaiian SNP sequence versus chromosome location (top panel). Reads closely linked to the *cov19* mutation are expected to consist of very low % Hawaiian SNP sequence. The normalized linkage score versus chromosome location (bottom panel). Red and gray columns within Chromosome 2 indicate regions significantly linked to the *cov19* Muv phenotype. The location of the *ufd-2* gene is also indicated (arrow). D) Diagram of the UFD-2 protein and the *ufd-2* gene. The allele *cov19* is a single nucleotide substitution causing a premature stop at codon 472. The deletion allele *tm1380* causes a frameshift and premature stop.

Supplemental Figure S2

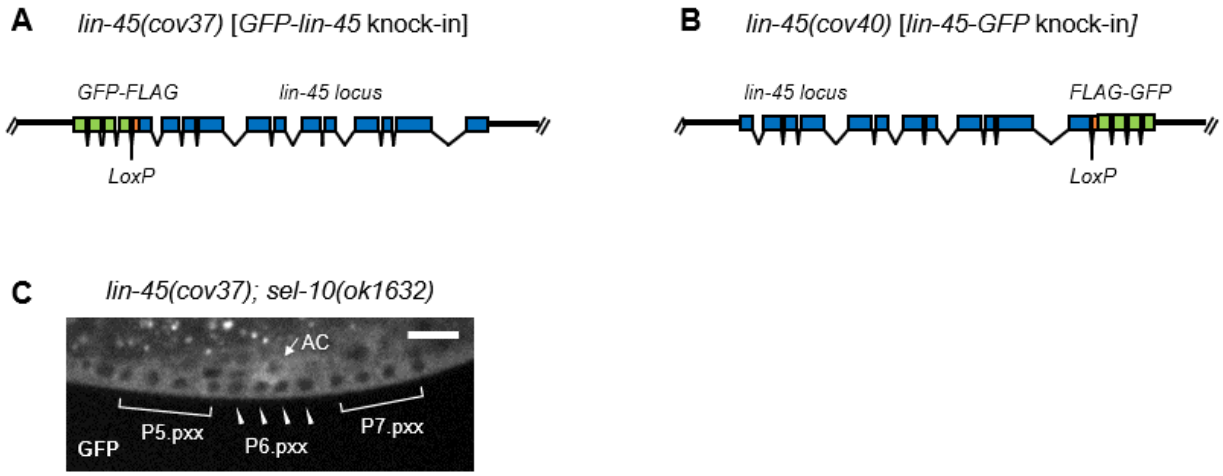

Figure 2.S2. Endogenous GFP-tagged LIN-45. A) Diagram of the *lin-45(cov37)* knock-in allele, encoding N-terminally tagged GFP-3xFLAG-LIN-45. B) Diagram of the *lin-45(cov40)* knock-in allele, encoding C-terminally tagged LIN-45-3xFLAG-GFP. C) Endogenous GFP-LIN-45, in the *sel-10(0)* mutant at the L3 larval stage; descendants of P5.p, P6.p, and P7.p are labeled P5.pxx, P6.pxx, and P7.pxx, respectively.

CHAPTER 3 - DISCUSSION AND CONCLUSIONS

In this work, we have found that UFD-2 participates in degradation of LIN-45 and LIN-45(V627E), as loss of UFD-2 results in partial stabilization of LIN-45 protein. In contrast to regulation by SEL-10, which requires solely a minimal CPD degron sequence, we found that regulation by UFD-2 requires multiple regions of LIN-45, including a 14-3-3 binding site as well as the N-terminus and C-terminus domains, but loss of UFD-2 does not stabilize the minimal CPD. One explanation of this novel regulation mechanism is that UFD-2 requires LIN-45 to be in a certain complex, subcellular compartment, or have a particular pattern of posttranslational modifications in order to be regulated. In addition to UFD-2, we have found that CDC-48, a known UFD-2-interacting protein, is required for LIN-45 protein degradation, since RNAi targeting CDC-48.1 and 2 results in stabilization of LIN-45 protein.

Our findings raise several questions regarding the regulation of LIN-45 by UFD-2 and CDC-48: i) is LIN-45 directly ubiquitinated by UFD-2? ii) does UFD-2 act as an E3 or E4 ubiquitin ligase regarding LIN-45? iii) is the role for UFD-2 in regulating Raf protein degradation conserved in humans? iv) what Raf complex is regulated by UFD-2?

i) Is LIN-45 ubiquitinated by UFD-2?

UFD-2 is known to have E3 and E4 ubiquitin ligase activities. Our experiments establish that UFD-2 is required for degradation of LIN-45. Based on this observation, we hypothesize that UFD-2 is responsible for ubiquitination of LIN-45. To test this possibility, we propose to examine the ubiquitination state of LIN-45 protein in *ufd-2* mutants.

In this work, we have generated an endogenous GFP-FLAG-LIN-45 allele. This allele can be used in immunoprecipitation of endogenous LIN-45 to determine its ubiquitination state. To assay LIN-45 ubiquitination, we can harvest worms treated with a proteasome inhibitor to prevent protein degradation, perform FLAG immunoprecipitation of LIN-45 with subsequent Western blotting and detection of ubiquitin with an anti-ubiquitin antibody. Using this method, we may be able to detect either mono-ubiquitination or poly-ubiquitin chains. If we identify a loss of ubiquitin chains bound to LIN-45 in a *ufd-2(0)* mutant, this would indicate that UFD-2 is able to ubiquitinate LIN-45.

Ubiquitin modifications are added at lysine residues. If we observe that ubiquitination of LIN-45 requires UFD-2, we could assay where UFD-2 attaches ubiquitin to LIN-45 by generating CRISPR alleles with mutated lysine residues, or generating these mutants in a bacterial system.

Immunoprecipitation of endogenous proteins from *C. elegans* can be technically challenging. If we are unable to pull down endogenous LIN-45, then an alternative approach would be to express the components in a bacterial system and assay ubiquitination activity *in vitro,* as done in Goh et al. 2008.

ii) Does UFD-2 act as E3 or E4 ubiquitin ligase regarding LIN-45?

UFD-2 has been found to have both E3 and E4 ubiquitin ligase activity. It is still unknown what type of ubiquitin ligase activity UFD-2 has regarding its regulation of LIN-45. One model to explain the regulation of LIN-45 by both SEL-10 and UFD-2 could be that SEL-10 acts as an E3 to mono-ubiquitinate LIN-45, allowing UFD-2 to act as an E4

and produce poly-ubiquitin chains. To address this possibility, we can assay *sel-10(0)* or double mutant *ufd-2(0); sel-10(0)* animals using the immunoprecipitation and ubiquitin detection assay described in the previous section. If *sel-10* and *ufd-2* both act as E3 ubiquitin ligases responsible for different ubiquitination sites, then we expect to see that the effect on ubiquitination is additive in the double mutant. Additionally, there may be differences in the effect of ufd-2 and sel-10 mutants on mono- or poly-ubiquitination. Mono-ubiquitination can be recognized as one lower molecular weight protein, whereas poly-ubiquitination produces a characteristic “ladder” of multiple high molecular weight proteins. If *ufd-2* only acts as an E4 ubiquitin ligase adding to a chain initiated by *sel-10*, then we expect that ubiquitin chain length in the double mutant will be unchanged from the *sel-10(0)* single mutant.

iii) Is the role for UFD-2 in regulating Raf protein degradation conserved in humans?

Although the Ras-Raf-MEK-ERK pathway is conserved from *C. elegans* to human, it is unknown whether the role for UFD-2 in regulating Raf protein degradation is conserved. Given the high conservation of UFD-2, we hypothesize that the human UFD-2 ortholog UBE4B also regulates protein degradation of BRAF. To test this possibility, we could culture human cells, use CRISPR or RNAi to knockdown UBE4B, and assay BRAF protein degradation using immunoprecipitation methods. This method has previously been used to show that human BRAF is ubiquitinated in human HEK 293 cells, and that FBXW7 is required (Saei et al. 2018). Due to this experiment being *in vivo,* a concern would be that ubiquitinated BRAF is being directed to the proteasome for degradation. Delivery of a proteasome inhibitor would be required to stop this activity.

If UBE4B is able to ubiquitinate BRAF, this would mean that the role of UFD-2 in regulation of LIN-45 is conserved from worm to human. The role of UBE4B in oncogenesis and other BRAF(V600E)-derived diseases could then be investigated. For example, if loss of UBE4B contributes to BRAF(V600E) cancers, then we may find its mutation occurs more frequently than expected by chance. We can survey available databases of cancer mutations, such as cBioPortal for Cancer Genomics (https://www.cbioportal.org/). Another approach would be to assay the effect of UBE4B knockdown on proliferation phenotypes of normal and melanoma cell lines carrying the BRAF(V600E) mutation.

iv) What Raf complex is regulated by UFD-2?

Our experiments found that UFD-2 requires a certain complex containing 14-3-3 proteins and the N- and C-terminus domains of LIN-45 for its activity. The exact complex containing LIN-45 required for UFD-2-mediated degradation is still unknown, as is the temporal point in LIN-45's activation cycle at which UFD-2 acts. It is also unknown if and what other proteins are required to degrade LIN-45 in a UFD-2-dependent manner. A co-immunoprecipitation experiment could be used to detect other proteins present in the LIN-45 complex being regulated, as well as other proteins required for the degradation activity of UFD-2. We could use CRIPSR/Cas9 to generate separate epitope tags of endogenous UFD-2, 14-3-3, and CDC-48.1/2, use ELISA to bind FLAG-tagged LIN-45, and assay which proteins are bound to LIN-45. If UFD-2 is detected in the presence of 14-3-3, it would indicate that UFD-2 is able to bind a complex of LIN-45 and 14-3-3. If UFD-2 is unable to bind to LIN-45 in this state, then this would imply that UFD-2 regulates LIN-45 at a point in its activation cycle where it is

not bound to 14-3-3. We could also use CRISPR/Cas9 to mutate endogenous LIN-45 to FLAG-tagged LIN-45(S312A) and LIN-45(S312A,S756A) and assay whether UFD-2 is able to bind to these mutant alleles. These results would indicate whether UFD-2 can regulate a form of LIN-45 that is not bound by 14-3-3.

Conclusion

In this work, we find that UFD-2 negatively regulates LIN-45 protein activity and levels through ubiquitin-mediated degradation. UFD-2-dependent degradation of LIN-45 requires the N- and C-terminus domains of LIN-45. We propose a model where UFD-2-dependent regulation of LIN-45 requires the S756 14-3-3 binding site. We also identify CDC-48.1 and 2, proteins known to interact with UFD-2, as negative regulators of LIN-45. These findings raise interesting questions about the role of ubiquitination in regulation of LIN-45 activity, as well as the relationship between UFD-2 and CDC-48.1 and 2 in this regulation. Further research is required to determine if mutations in UFD-2 contribute to melanoma or other cancers, and what the implications would be for future therapeutics.

REFERENCES

Abdus-Saboor, I., Mancuso, V.P., Murray, J.I., Palozola, K., Norris, C., Hall, D.H., Howell, K., Huang, K., and Sundaram, M.V. (2011). Notch and Ras promote sequential steps of excretory tube development in C. elegans. Development *138*, 3545-3555. 10.1242/dev.068148.

Ackermann, L., Schell, M., Pokrzywa, W., Kevei, É., Gartner, A., Schumacher, B., and Hoppe, T. (2016). E4 ligase-specific ubiquitination hubs coordinate DNA double-strand-break repair and apoptosis. Nat Struct Mol Biol *23*, 995-1002. 10.1038/nsmb.3296.

Baek, G.H., Cheng, H., Choe, V., Bao, X., Shao, J., Luo, S., and Rao, H. (2013). Cdc48: a swiss army knife of cell biology. J Amino Acids *2013*, 183421. 10.1155/2013/183421.

Block, C., Janknecht, R., Herrmann, C., Nassar, N., and Wittinghofer, A. (1996). Quantitative structure-activity analysis correlating Ras/Raf interaction in vitro to Raf activation in vivo. Nat Struct Biol *3*, 244-251. 10.1038/nsb0396-244.

Böhm, S., Lamberti, G., Fernández-Sáiz, V., Stapf, C., and Buchberger, A. (2011). Cellular functions of Ufd2 and Ufd3 in proteasomal protein degradation depend on Cdc48 binding. Mol Cell Biol *31*, 1528-1539. 10.1128/MCB.00962-10.

Chong, H., Lee, J., and Guan, K.L. (2001). Positive and negative regulation of Raf kinase activity and function by phosphorylation. EMBO J *20*, 3716-3727. 10.1093/emboj/20.14.3716.

Chung, E., and Kondo, M. (2011). Role of Ras/Raf/MEK/ERK signaling in physiological hematopoiesis and leukemia development. Immunol Res *49*, 248-268. 10.1007/s12026-010-8187-5.

Clark, S.G., Stern, M.J., and Horvitz, H.R. (1992). C. elegans cell-signalling gene sem-5 encodes a protein with SH2 and SH3 domains. Nature *356*, 340-344. 10.1038/356340a0.

Connell, P., Ballinger, C.A., Jiang, J., Wu, Y., Thompson, L.J., Höhfeld, J., and Patterson, C. (2001). The co-chaperone CHIP regulates protein triage decisions mediated by heat-shock proteins. Nat Cell Biol *3*, 93-96. 10.1038/35050618.

Conte, D., MacNeil, L.T., Walhout, A.J.M., and Mello, C.C. (2015). RNA Interference in Caenorhabditis elegans. Curr Protoc Mol Biol *109*, 26.23.21-26.23.30. 10.1002/0471142727.mb2603s109.

Damsky, W.E., and Bosenberg, M. (2017). Melanocytic nevi and melanoma: unraveling a complex relationship. Oncogene *36*, 5771-5792. 10.1038/onc.2017.189.

Das, A.K., Cohen, P.W., and Barford, D. (1998). The structure of the tetratricopeptide repeats of protein phosphatase 5: implications for TPR-mediated protein-protein interactions. EMBO J *17*, 1192-1199. 10.1093/emboj/17.5.1192.

Davies, H., Bignell, G.R., Cox, C., Stephens, P., Edkins, S., Clegg, S., Teague, J., Woffendin, H., Garnett, M.J., Bottomley, W., et al. (2002). Mutations of the BRAF gene in human cancer. Nature *417*, 949-954. 10.1038/nature00766.

de la Cova, C., and Greenwald, I. (2012). SEL-10/Fbw7-dependent negative feedback regulation of LIN-45/Braf signaling in C. elegans via a conserved phosphodegron. Genes Dev *26*, 2524-2535. 10.1101/gad.203703.112.

de la Cova, C., Townley, R., Regot, S., and Greenwald, I. (2017). A Real-Time Biosensor for ERK Activity Reveals Signaling Dynamics during C. elegans Cell Fate Specification. Dev Cell *42*, 542-553.e544. 10.1016/j.devcel.2017.07.014.

de la Cova, C.C., Townley, R., and Greenwald, I. (2020). Negative feedback by conserved kinases patterns the degradation of. Development *147*. 10.1242/dev.195941.

Deng, Y., Luo, K.L., Shaye, D.D., and Greenwald, I. (2019). A Screen of the Conserved Kinome for Negative Regulators of LIN-12 Negative Regulatory Region (''NRR'')-Missense Activity in. G3 (Bethesda) *9*, 3567-3574. 10.1534/g3.119.400471.

Dhillon, A.S., Meikle, S., Yazici, Z., Eulitz, M., and Kolch, W. (2002). Regulation of Raf-1 activation and signalling by dephosphorylation. EMBO J *21*, 64-71. 10.1093/emboj/21.1.64.

Dickinson, D.J., and Goldstein, B. (2016). CRISPR-Based Methods for Caenorhabditis elegans Genome Engineering. Genetics *202*, 885-901. 10.1534/genetics.115.182162.

Dougherty, M.K., Müller, J., Ritt, D.A., Zhou, M., Zhou, X.Z., Copeland, T.D., Conrads, T.P., Veenstra, T.D., Lu, K.P., and Morrison, D.K. (2005). Regulation of Raf-1 by direct feedback phosphorylation. Mol Cell *17*, 215-224. 10.1016/j.molcel.2004.11.055.

Eisenhardt, A.E., Sprenger, A., Röring, M., Herr, R., Weinberg, F., Köhler, M., Braun, S., Orth, J., Diedrich, B., Lanner, U., et al. (2016). Phospho-proteomic analyses of B-Raf protein complexes reveal new regulatory principles. Oncotarget *7*, 26628-26652. 10.18632/oncotarget.8427.

Ferguson, E.L., and Horvitz, H.R. (1985). Identification and characterization of 22 genes that affect the vulval cell lineages of the nematode Caenorhabditis elegans. Genetics *110*, 17-72.

Frøkjær-Jensen, C., Davis, M.W., Sarov, M., Taylor, J., Flibotte, S., LaBella, M., Pozniakovsky, A., Moerman, D.G., and Jorgensen, E.M. (2014). Random and

targeted transgene insertion in Caenorhabditis elegans using a modified Mos1 transposon. Nat Methods *11*, 529-534. 10.1038/nmeth.2889.

Garnett, M.J., Rana, S., Paterson, H., Barford, D., and Marais, R. (2005). Wild-type and mutant B-RAF activate C-RAF through distinct mechanisms involving heterodimerization. Mol Cell *20*, 963-969. 10.1016/j.molcel.2005.10.022.

Goh, A.M., Walters, K.J., Elsasser, S., Verma, R., Deshaies, R.J., Finley, D., and Howley, P.M. (2008). Components of the ubiquitin-proteasome pathway compete for surfaces on Rad23 family proteins. BMC Biochem *9*, 4. 10.1186/1471-2091-9-4.

Han, M., Golden, A., Han, Y., and Sternberg, P.W. (1993). C. elegans lin-45 raf gene participates in let-60 ras-stimulated vulval differentiation. Nature *363*, 133-140. 10.1038/363133a0.

Hatakeyama, S., and Nakayama, K.I. (2003). U-box proteins as a new family of ubiquitin ligases. Biochem Biophys Res Commun *302*, 635-645. 10.1016/s0006-291x(03)00245-6.

Hellerschmied, D., Roessler, M., Lehner, A., Gazda, L., Stejskal, K., Imre, R., Mechtler, K., Dammermann, A., and Clausen, T. (2018). UFD-2 is an adaptor-assisted E3 ligase targeting unfolded proteins. Nat Commun *9*, 484. 10.1038/s41467-018-02924-7.

Hoppe, T., Cassata, G., Barral, J.M., Springer, W., Hutagalung, A.H., Epstein, H.F., and Baumeister, R. (2004). Regulation of the myosin-directed chaperone UNC-45 by a novel E3/E4-multiubiquitylation complex in C. elegans. Cell *118*, 337-349. 10.1016/j.cell.2004.07.014.

Houben, R., Vetter-Kauczok, C.S., Ortmann, S., Rapp, U.R., Broecker, E.B., and Becker, J.C. (2008). Phospho-ERK staining is a poor indicator of the mutational status of BRAF and NRAS in human melanoma. J Invest Dermatol *128*, 2003-2012. 10.1038/jid.2008.30.

Hsu, V., Zobel, C.L., Lambie, E.J., Schedl, T., and Kornfeld, K. (2002). Caenorhabditis elegans lin-45 raf is essential for larval viability, fertility and the induction of vulval cell fates. Genetics *160*, 481-492.

Janiesch, P.C., Kim, J., Mouysset, J., Barikbin, R., Lochmüller, H., Cassata, G., Krause, S., and Hoppe, T. (2007). The ubiquitin-selective chaperone CDC-48/p97 links myosin assembly to human myopathy. Nat Cell Biol *9*, 379-390. 10.1038/ncb1554.

Jung, T., Catalgol, B., and Grune, T. (2009). The proteasomal system. Mol Aspects Med *30*, 191-296. 10.1016/j.mam.2009.04.001.

Kaletta, T., and Hengartner, M.O. (2006). Finding function in novel targets: C. elegans

as a model organism. Nat Rev Drug Discov *5*, 387-398. 10.1038/nrd2031.

Kamath, R.S., and Ahringer, J. (2003). Genome-wide RNAi screening in Caenorhabditis elegans. Methods *30*, 313-321. 10.1016/s1046-2023(03)00050-1.

Karnoub, A.E., and Weinberg, R.A. (2008). Ras oncogenes: split personalities. Nat Rev Mol Cell Biol *9*, 517-531. 10.1038/nrm2438.

Kiel, C., Benisty, H., Lloréns-Rico, V., and Serrano, L. (2016). The yin-yang of kinase activation and unfolding explains the peculiarity of Val600 in the activation segment of BRAF. Elife *5*, e12814. 10.7554/eLife.12814.

Kim, W., Underwood, R.S., Greenwald, I., and Shaye, D.D. (2018). OrthoList 2: A New Comparative Genomic Analysis of Human and. Genetics *210*, 445-461. 10.1534/genetics.118.301307.

Koegl, M., Hoppe, T., Schlenker, S., Ulrich, H.D., Mayer, T.U., and Jentsch, S. (1999). A novel ubiquitination factor, E4, is involved in multiubiquitin chain assembly. Cell *96*, 635-644. 10.1016/s0092-8674(00)80574-7.

Kondo, Y., Ognjenović, J., Banerjee, S., Karandur, D., Merk, A., Kulhanek, K., Wong, K., Roose, J.P., Subramaniam, S., and Kuriyan, J. (2019). Cryo-EM structure of a dimeric B-Raf:14-3-3 complex reveals asymmetry in the active sites of B-Raf kinases. Science *366*, 109-115. 10.1126/science.aay0543.

Köhler, M., and Brummer, T. (2016). B-Raf activation loop phosphorylation revisited. Cell Cycle *15*, 1171-1173. 10.1080/15384101.2016.1159111.

Lavoie, H., and Therrien, M. (2015). Regulation of RAF protein kinases in ERK signalling. Nat Rev Mol Cell Biol *16*, 281-298. 10.1038/nrm3979.

Leicht, D.T., Balan, V., Kaplun, A., Singh-Gupta, V., Kaplun, L., Dobson, M., and Tzivion, G. (2007). Raf kinases: function, regulation and role in human cancer. Biochim Biophys Acta *1773*, 1196-1212. 10.1016/j.bbamcr.2007.05.001.

Logue, J.S., and Morrison, D.K. (2012). Complexity in the signaling network: insights from the use of targeted inhibitors in cancer therapy. Genes Dev *26*, 641-650. 10.1101/gad.186965.112.

Margolis, B., and Skolnik, E.Y. (1994). Activation of Ras by receptor tyrosine kinases. J Am Soc Nephrol *5*, 1288-1299. 10.1681/ASN.V561288.

Mercer, K., Giblett, S., Green, S., Lloyd, D., DaRocha Dias, S., Plumb, M., Marais, R., and Pritchard, C. (2005). Expression of endogenous oncogenic V600EB-raf induces proliferation and developmental defects in mice and transformation of primary fibroblasts. Cancer Res *65*, 11493-11500. 10.1158/0008-5472.CAN-05-2211.

Muslin, A.J., Tanner, J.W., Allen, P.M., and Shaw, A.S. (1996). Interaction of 14-3-3 with signaling proteins is mediated by the recognition of phosphoserine. Cell *84*, 889-897. 10.1016/s0092-8674(00)81067-3.

Pandit, B., Sarkozy, A., Pennacchio, L.A., Carta, C., Oishi, K., Martinelli, S., Pogna, E.A., Schackwitz, W., Ustaszewska, A., Landstrom, A., et al. (2007). Gain-of-function RAF1 mutations cause Noonan and LEOPARD syndromes with hypertrophic cardiomyopathy. Nat Genet *39*, 1007-1012. 10.1038/ng2073.

Papaevgeniou, N., and Chondrogianni, N. (2014). The ubiquitin proteasome system in Caenorhabditis elegans and its regulation. Redox Biol *2*, 333-347. 10.1016/j.redox.2014.01.007.

Park, E., Rawson, S., Li, K., Kim, B.W., Ficarro, S.B., Pino, G.G., Sharif, H., Marto, J.A., Jeon, H., and Eck, M.J. (2019). Architecture of autoinhibited and active BRAF-MEK1-14-3-3 complexes. Nature *575*, 545-550. 10.1038/s41586-019-1660-y.

Passmore, L.A., and Barford, D. (2004). Getting into position: the catalytic mechanisms of protein ubiquitylation. Biochem J *379*, 513-525. 10.1042/BJ20040198.

Regot, S., Hughey, J.J., Bajar, B.T., Carrasco, S., and Covert, M.W. (2014). High-sensitivity measurements of multiple kinase activities in live single cells. Cell *157*, 1724-1734. 10.1016/j.cell.2014.04.039.

Richly, H., Rape, M., Braun, S., Rumpf, S., Hoege, C., and Jentsch, S. (2005). A series of ubiquitin binding factors connects CDC48/p97 to substrate multiubiquitylation and proteasomal targeting. Cell *120*, 73-84. 10.1016/j.cell.2004.11.013.

Ritt, D.A., Monson, D.M., Specht, S.I., and Morrison, D.K. (2010). Impact of feedback phosphorylation and Raf heterodimerization on normal and mutant B-Raf signaling. Mol Cell Biol *30*, 806-819. 10.1128/MCB.00569-09.

Robert, X., and Gouet, P. (2014). Deciphering key features in protein structures with the new ENDscript server. Nucleic Acids Res 42, W320-324. 10.1093/nar/gku316.

Rushworth, L.K., Hindley, A.D., O'Neill, E., and Kolch, W. (2006). Regulation and role of Raf-1/B-Raf heterodimerization. Mol Cell Biol *26*, 2262-2272. 10.1128/MCB.26.6.2262-2272.2006.

Saei, A., Palafox, M., Benoukraf, T., Kumari, N., Jaynes, P.W., Iyengar, P.V., Muñoz-Couselo, E., Nuciforo, P., Cortés, J., Nötzel, C., et al. (2018). Loss of USP28-mediated BRAF degradation drives resistance to RAF cancer therapies. J Exp Med *215*, 1913-1928. 10.1084/jem.20171960.

Sallee, M.D., and Greenwald, I. (2015). Dimerization-driven degradation of C. elegans and human E proteins. Genes Dev *29*, 1356-1361. 10.1101/gad.261917.115.

Schmitz, C., Kinge, P., and Hutter, H. (2007). Axon guidance genes identified in a large-

scale RNAi screen using the RNAi-hypersensitive Caenorhabditis elegans strain nre-1(hd20) lin-15b(hd126). Proc Natl Acad Sci U S A *104*, 834-839. 10.1073/pnas.0510527104.

Schubbert, S., Shannon, K., and Bollag, G. (2007). Hyperactive Ras in developmental disorders and cancer. Nat Rev Cancer *7*, 295-308. 10.1038/nrc2109.

Shin, H., and Reiner, D.J. (2018). The Signaling Network Controlling C. elegans Vulval Cell Fate Patterning. J Dev Biol *6*. 10.3390/jdb6040030.

Siegel, R.L., Miller, K.D., and Jemal, A. (2020). Cancer statistics, 2020. CA Cancer J Clin *70*, 7-30. 10.3322/caac.21590.

Sternberg, P.W., Golden, A., and Han, M. (1993). Role of a raf proto-oncogene during Caenorhabditis elegans vulval development. Philos Trans R Soc Lond B Biol Sci *340*, 259-265. 10.1098/rstb.1993.0066.

Stiernagle, T. (2006). Maintenance of C. elegans. WormBook, 1-11. 10.1895/wormbook.1.101.1.

Sundaram, M.V. (2013). Canonical RTK-Ras-ERK signaling and related alternative pathways. WormBook, 1-38. 10.1895/wormbook.1.80.2.

Tan, P.B., Lackner, M.R., and Kim, S.K. (1998). MAP kinase signaling specificity mediated by the LIN-1 Ets/LIN-31 WH transcription factor complex during C. elegans vulval induction. Cell *93*, 569-580. 10.1016/s0092-8674(00)81186-1.

Udell, C.M., Rajakulendran, T., Sicheri, F., and Therrien, M. (2011). Mechanistic principles of RAF kinase signaling. Cell Mol Life Sci *68*, 553-565. 10.1007/s00018-010-0520-6.

Underwood, R.S., Deng, Y., and Greenwald, I. (2017). Integration of EGFR and LIN-12/Notch Signaling by LIN-1/Elk1, the Cdk8 Kinase Module, and SUR-2/Med23 in Vulval Precursor Cell Fate Patterning in. Genetics *207*, 1473-1488. 10.1534/genetics.117.300192.

Venesio, T., Chiorino, G., Balsamo, A., Zaccagna, A., Petti, C., Scatolini, M., Pisacane, A., Sarotto, I., Picciotto, F., and Risio, M. (2008). In melanocytic lesions the fraction of BRAF V600E alleles is associated with sun exposure but unrelated to ERK phosphorylation. Mod Pathol *21*, 716-726. 10.1038/modpathol.2008.41.

Welcker, M., and Clurman, B.E. (2008). FBW7 ubiquitin ligase: a tumour suppressor at the crossroads of cell division, growth and differentiation. Nat Rev Cancer *8*, 83-93. 10.1038/nrc2290.

Yoon, S., and Seger, R. (2006). The extracellular signal-regulated kinase: multiple substrates regulate diverse cellular functions. Growth Factors *24*, 21-44. 10.1080/02699050500284218.

Yumimoto, K., and Nakayama, K.I. (2020). Recent insight into the role of FBXW7 as a tumor suppressor. Semin Cancer Biol *67*, 1-15. 10.1016/j.semcancer.2020.02.017.

Zhang, X., and Greenwald, I. (2011). Spatial regulation of lag-2 transcription during vulval precursor cell fate patterning in Caenorhabditis elegans. Genetics *188*, 847-858. 10.1534/genetics.111.128389.

APPENDIX A:

ALIGNMENT OF ARAF, BRAF, CRAF, AND LIN-45

Conserved residues are marked in dark red highlighting. Functionally similar residues are marked in red font. Secondary structural elements are labeled above the corresponding sequence. Sequences were aligned using Clustal Omega and structural elements were marked using ESPript (Robert & Gouet 2014).

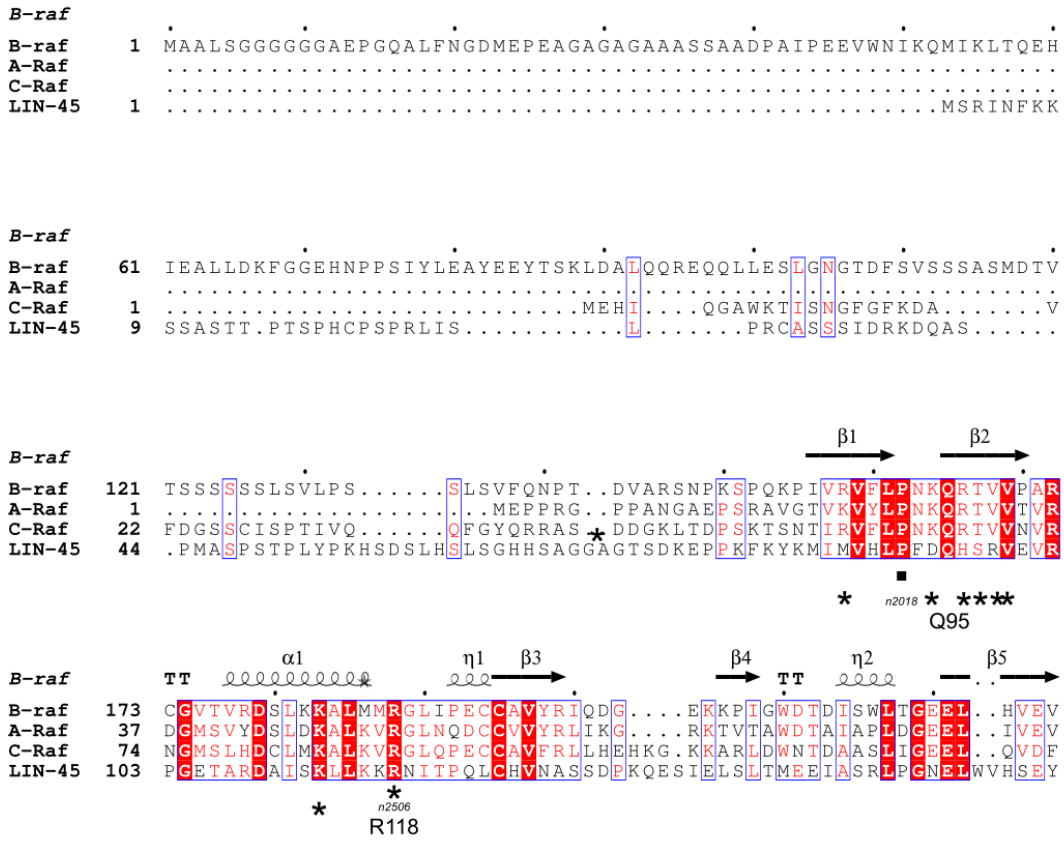
B-raf
B-raf 1 MAALSGGGGGGAEPGQALFNGDMEPEAGAGAGAAASSAADPAIPEEVWNIKQMIKLTQEH
A-Raf
C-Raf
LIN-45 1 .....MSRINFKK
B-raf
B-raf 61 IEALLDKFGGEHNPPSIYLEAYEEYTSKLDALQQREQQLLESLGNGTDFSVSSSASMDTV
A-Raf
C-Raf 1 .....MEHI....QGAWKTISNGFGFKDA.....V
LIN-45 9 SSASTT.PTSPHCPSPRLIS.....L.....PRCASSSIDRKDQAS.....
β1
β2
B-raf
B-raf 121 TSSSSSSLSVLPS.....SLSVFQNPT..DVARSNPKSPQKPIVRVFLPNKQRTVVPAR
A-Raf 1 .....MEPPRG..PPANGAEPSRAVGTVKVYLPNKQRTVVTVR
C-Raf 22 FDGSSCISPTIVQ.....QFGYQRRAS..DDGKLTDPSKTSNTIRVFLPNKQRTVVNVR
LIN-45 44 .PMASPSTPLYPKHSDSLHSLSGHHSAGGAGTSDKEPPKFKYKMIMVHLPFDQHSRVEVR
n2018
Q95
α1
η1
β3
β4
η2
β5
B-raf
TT
TT
B-raf 173 CGVTVRDSLKKALMMRGLIPECCAVYRIQDG....EKKPIGWDTDISWLTGEEL..HVEV
A-Raf 37 DGMSVYDSLDKALKVRGLNQDCCVVYRLIKG....RKTVTAWDTAIAPLDGEEL..IVEV
C-Raf 74 NGMSLHDCLMKALKVRGLQPECCAVFRLLHEHKG.KKARLDWNTDAASLIGEEL..QVDF
LIN-45 103 PGETARDAISKLLKKRNITPQLCHVNASSDPKQESIELSLTMEEIASRLPGNELWVHSEY
n2506
R118
B-raf
B-raf 227 LENVPLTTHNFVRKTFFTLAFCDFCRKL.LFQGFRCQTCGYKFHQRCSTEVPLMCVNYDQ
A-Raf 91 LEDVPLTMHNFVRKTFFSLAFCDFCLKF.LFHGFRCQTCGYKFHQHCSSKVPTVCVDMST
C-Raf 131 LDHVPLTTHNFARKTFLKLAFCDICQKF.LLNGFRCQTCGYKFHEHCSTKVPTMCVDWSN
LIN-45 163 LNTVSSIKHAIVRRTFIPPKSCDVCNNPIWMMGFRCEFCQFKFHQRCSSFAPLYCDLLQS
B-raf
B-raf 286 LDL...LFVSKFFEHHPIP.....QEEASLAETALTSGSSPSAPASDSIGPQILT.....
A-Raf 150 NRQ...|..QFYHSV..QD.....L.....SGGSRQHEAPSNRPLNELLTPQ..GPSP..
C-Raf 190 IRQ...LLL.FPNST..IG.....D.....SGV.PALPSLTMRRMRESVSRM..PVSS..
LIN-45 223 VPKNEDLVKELFGIASQVEGPDRSVAEIVLANLAPTSGQSPAATPDSSHPDL.....TS
B-raf
B-raf 333 ..SPSPSKSIPIPQPFRP...ADEDHRNQFGQRDRSSSAPNVHINTIEPVNIDDLIRDQG
A-Raf 188 ....RTQHCDPEHFP.....FPAPANAPLQRIRSTSTPNVHMVSTTAPMDSNLIQLTG
C-Raf 229 ....QHRYSTPHAFTFNT...SSPSSEGSLSQRQRSTSTPNVHMVSTTLPVDSRMIEDAI
LIN-45 277 IK..RTGGVKRHPMAVSPQNETSQLSPSGPYPRDRSSSAPNINAINDEATVQHNQRILDA
B-raf
B-raf 388 F.....RG....D.....
A-Raf 237 Q.....SF....STDAAGS.....RGGSD.....
C-Raf 282 R.....SH....SE.....
LIN-45 335 LEAQRLEEESRDKTGSLLSTQARHRPHFQSGHILSGARMNRLHPLVDCTPLGSNSPSSTC

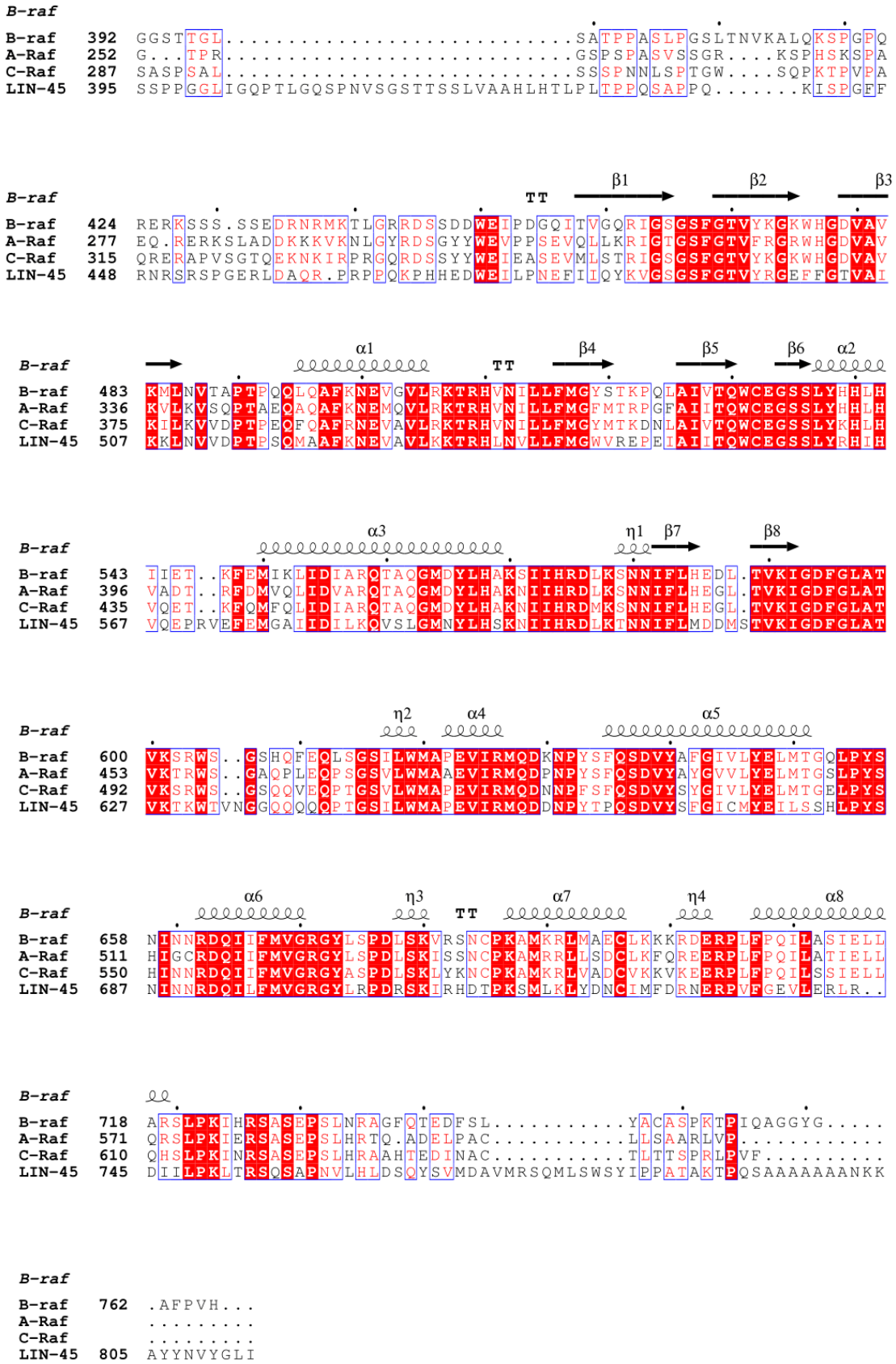
B-raf
B-raf 392 GGSTTGL.....SATPPASLPGSLTNVKALQKSPGPQ
A-Raf 252 G...TPR.....GSPSPASVSSGR....KSPHSKSPA
C-Raf 287 SASPSAL.....SSSPNNLSPTGW....SQPKTPVPA
LIN-45 395 SSPPGGLIGQPTLGQSPNVSGSTTSSLVAAHLHTLPLTPPQSAPPQ.....KISPGFF
B-raf
TT
β1
β2
β3
B-raf 424 RERKSSS.SSEDRNRMKTLGRRDSSDDWEIPDGQITVGQRIGSGSFGTVYKGKWHGDVAV
A-Raf 277 EQ.RERKSLADDKKKVKNLGYRDSGYYWEVPPSEVQLLKRIGTGSFGTVFRGRWHGDVAV
C-Raf 315 QRERAPVSGTQEKNKIRPRGQRDSSYYWEIEASEVMLSTRIGSGSFGTVYKGKWHGDVAV
LIN-45 448 RNRSRSPGERLDAQR.PRPPQKPHHEDWEILPNEFIIQYKVGSGSFGTVYRGEFFGTVAI
B-raf
α1
TT
β4
β5
β6
α2
B-raf 483 KMLNVTAPTPQQLQAFKNEVGVLRKTRHVNILLFMGYSTKPQLAIVTQWCEGSSLYHHLH
A-Raf 336 KVLKVSQPTAEQAQAFKNEMQVLRKTRHVNILLFMGFMTRPGFAIITQWCEGSSLYHHLH
C-Raf 375 KILKVVDPTPEQFQAFRNEVAVLRKTRHVNILLFMGYMTKDNLAIVTQWCEGSSLYKHLH
LIN-45 507 KKLNVVDPTPSQMAAFKNEVAVLKKTRHLNVLLFMGWVREPEIAIITQWCEGSSLYRHIH
B-raf
α3
η1
β7
β8
B-raf 543 IIET..KFEMIKLIDIARQTAQGMDYLHAKSIIHRDLKSNNIFLHEDL.TVKIGDFGLAT
A-Raf 396 VADT..RFDMVQLIDVARQTAQGMDYLHAKNIIHRDLKSNNIFLHEGL.TVKIGDFGLAT
C-Raf 435 VQET..KFQMFQLIDIARQTAQGMDYLHAKNIIHRDMKSNNIFLHEGL.TVKIGDFGLAT
LIN-45 567 VQEPRVEFEMGAIIDILKQVSLGMNYLHSKNIIHRDLKTNNIFLMDDMSTVKIGDFGLAT
B-raf
η2
α4
α5
B-raf 600 VKSRWS..GSHQFEQLSGSILWMAPEVIRMQDKNPYSFQSDVYAFGIVLYELMTGQLPYS
A-Raf 453 VKTRWS..GAQPLEQPSGSVLWMAAEVIRMQDPNPYSFQSDVYAYGVVLYELMTGSLPYS
C-Raf 492 VKSRWS..GSQQVEQPTGSVLWMAPEVIRMQDNNPFSFQSDVYSYGIVLYELMTGELPYS
LIN-45 627 VKTKWTVNGGQQQQQPTGSILWMAPEVIRMQDDNPYTPQSDVYSFGICMYEILSSHLPYS
B-raf
α6
η3
TT
α7
η4
α8
B-raf 658 NINNRDQIIFMVGRGYLSPDLSKVRSNCPKAMKRLMAECLKKKRDERPLFPQILASIELL
A-Raf 511 HIGCRDQIIFMVGRGYLSPDLSKISSNCPKAMRRLLSDCLKFQREERPLFPQILATIELL
C-Raf 550 HINNRDQIIFMVGRGYASPDLSKLYKNCPKAMKRLVADCVKKVKEERPLFPQILSSIELL
LIN-45 687 NINNRDQILFMVGRGYLRPDRSKIRHDTPKSMLKLYDNCIMFDRNERPVFGEVLERLR..
B-raf
B-raf 718 ARSLPKIHRSASEPSLNRAGFQTEDFSL.....YACASPKTPIQAGGYG.....
A-Raf 571 QRSLPKIERSASEPSLHRTQ.ADELPAC.....LLSAARLVP.....
C-Raf 610 QHSLPKINRSASEPSLHRAAHTEDINAC.....TLTTSPRLPVF.....
LIN-45 745 DIILPKLTRSQSAPNVLHLDSQYSVMDAVMRSQMLSWSYIPPATAKTPQSAAAAAAANKK
B-raf
B-raf 762 .AFPVH...
A-Raf .....
C-Raf .....
LIN-45 805 AYYNVYGLI

APPENDIX B:

ALIGNMENT OF P97,CDC-48.1, AND CDC-48.2

Conserved residues are marked in dark red highlighting. Functionally similar residues are marked in red font. Secondary structural elements are labeled above the corresponding sequence. Sequences were aligned using Clustal Omega and structural elements were marked using ESPript (Robert & Gouet 2014).

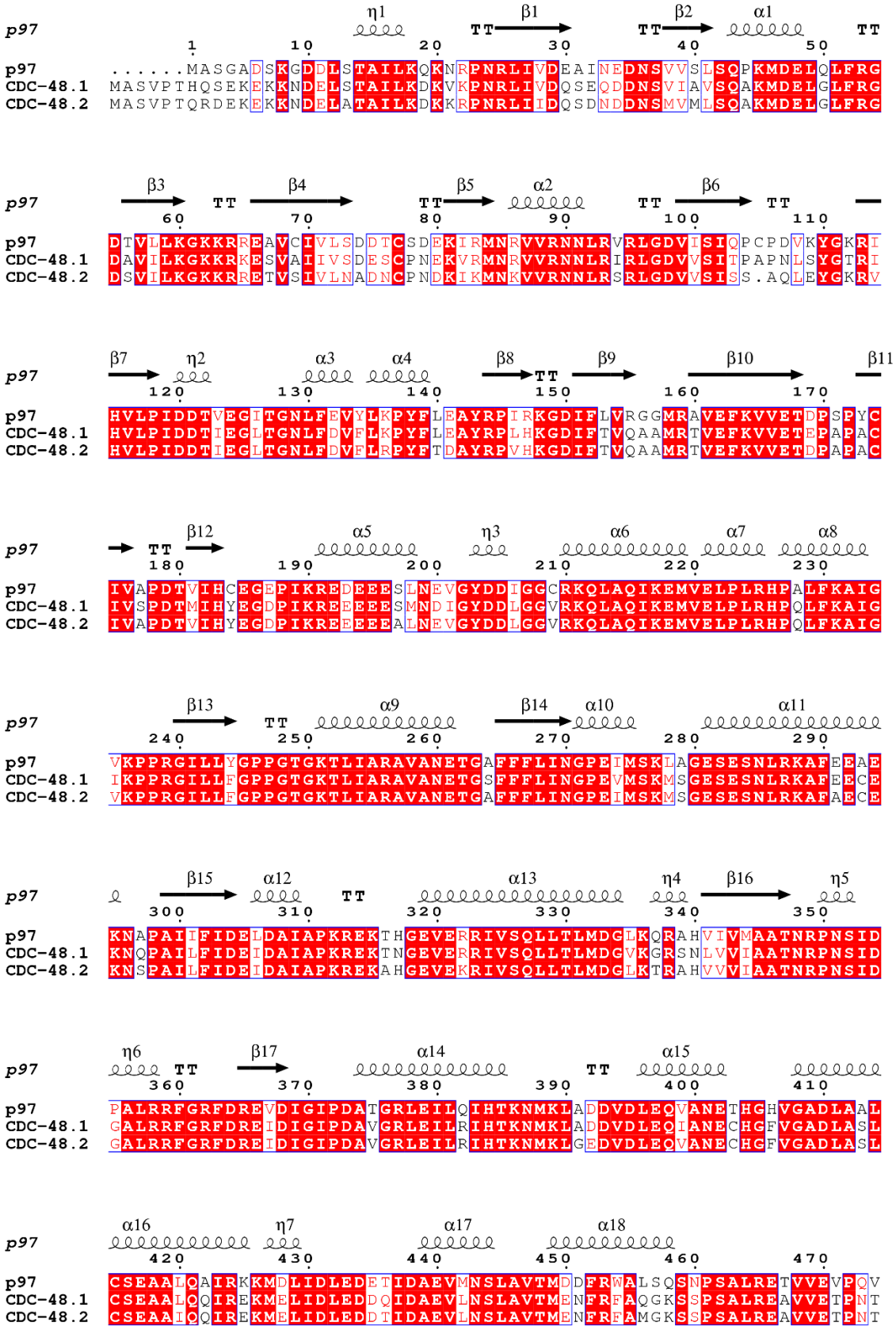
p97
CDC-48.1
CDC-48.2

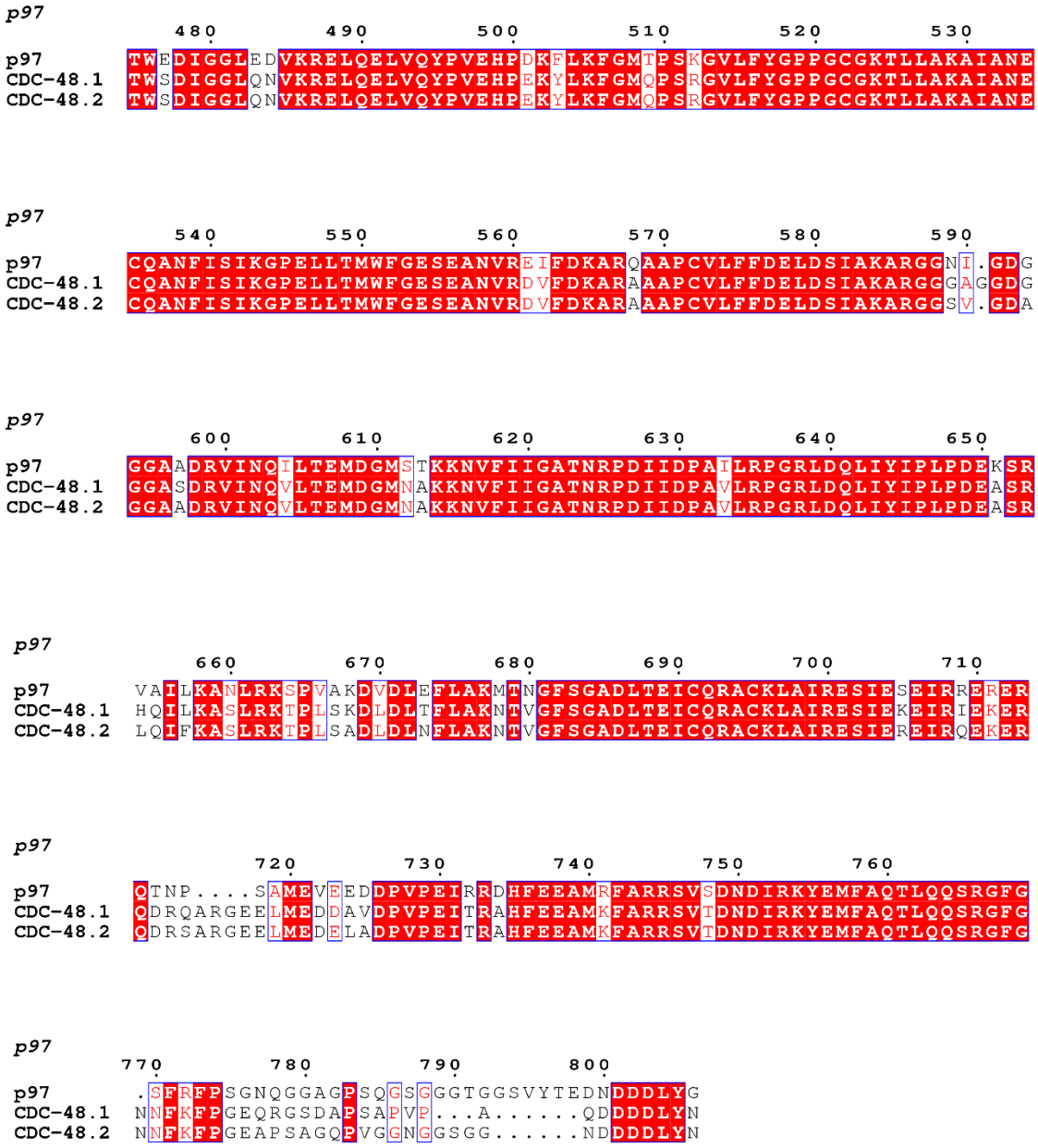
p97
480 490 500 510 520 530
p97 TWEDIGGLEDVKRELQELVQYPVEHPDKFLKFGMTPSKGVLFYGPPGCGKTLLAKAIANE
CDC-48.1 TWSDIGGLQNVKRELQELVQYPVEHPEKYLKFGMQPSRGVLFYGPPGCGKTLLAKAIANE
CDC-48.2 TWSDIGGLQNVKRELQELVQYPVEHPEKYLKFGMQPSRGVLFYGPPGCGKTLLAKAIANE
p97
540 550 560 570 580 590
p97 CQANFISIKGPELLTMWFGESEANVREIFDKARQAAPCVLFFDELDSIAKARGGNI.GDG
CDC-48.1 CQANFISIKGPELLTMWFGESEANVRDVFDKARAAAPCVLFFDELDSIAKARGGGAGGDG
CDC-48.2 CQANFISIKGPELLTMWFGESEANVRDVFDKARAAAPCVLFFDELDSIAKARGGSV.GDA
p97
600 610 620 630 640 650
p97 GGAADRVINQILTEMDGMSTKKNVFIIGATNRPDIIDPAILRPGRLDQLIYIPLPDEKSR
CDC-48.1 GGASDRVINQVLTEMDGMNAKKNVFIIGATNRPDIIDPAVLRPGRLDQLIYIPLPDEASR
CDC-48.2 GGAADRVINQVLTEMDGMNAKKNVFIIGATNRPDIIDPAVLRPGRLDQLIYIPLPDEASR
p97
660 670 680 690 700 710
p97 VAILKANLRKSPVAKDVDLEFLAKMTNGFSGADLTEICQRACKLAIRESIESEIRRERER
CDC-48.1 HQILKASLRKTPLSKDLDLTFLAKNTVGFSGADLTEICQRACKLAIRESIEKEIRIEKER
CDC-48.2 LQIFKASLRKTPLSADLDLNFLAKNTVGFSGADLTEICQRACKLAIRESIEREIRQEKER
p97
720 730 740 750 760
p97 QTNP....SAMEVEEDDPVPEIRRDHFEEAMRFARRSVSDNDIRKYEMFAQTLQQSRGFG
CDC-48.1 QDRQARGEELMEDDAVDPVPEITRAHFEEAMKFARRSVTDNDIRKYEMFAQTLQQSRGFG
CDC-48.2 QDRSARGEELMEDELADPVPEITRAHFEEAMKFARRSVTDNDIRKYEMFAQTLQQSRGFG
p97
770 780 790 800
p97 .SFRFPSGNQGGAGPSQGSGGGTGGSVYTEDNDDDLYG
CDC-48.1 NNFKFPGEQRGSDAPSAPVP...A......QDDDDLYN
CDC-48.2 NNFKFPGEAPSAGQPVGGNGGSGG......NDDDDLYN

APPENDIX C:

TABLE OF GENES TESTED USING RNAI

Genes known to interact with UFD-2, LIN-45, or other portions of the ubiquitin-proteasome system were tested for their ability to stabilize YFP-LIN-45 in the descendants of P6.p.

Tested genes	% Stabilized in P6.p descendants	Justification for testing (pathway or type of protein)
uba-1	0/14 (0%)	E1 ubiquitin ligase
ubc-9	0/11 (0%)	E2 ubiquitin ligase
ubc-12	0/14 (0%)	E2 ubiquitin ligase
apc-11	0/25 (0%)	E3 ubiquitin ligase
fzr-1	0/28 (0%)	E3 ubiquitin ligase
fzy-1	0/24 (0%)	E3 ubiquitin ligase
lin-23	0/45 (0%)	E3 ubiquitin ligase
lin-41	0/48 (0%)	E3 ubiquitin ligase
rbx-1	1/56 (2%)	E3 ubiquitin ligase
rbx-1/2	0/28 (0%)	E3 ubiquitin ligase
rfp-1	0/20 (0%)	E3 ubiquitin ligase
wwp-1	0/19 (0%)	E3 ubiquitin ligase
cul-1	0/28 (0%)	E3 ubiquitin ligase
cyn-4/mog-6	1/28 (4%)	U-box E3/E4 ubiquitin ligase (similar to UFD-2)
prp-19	0/14 (0%)	U-box E3/E4 ubiquitin ligase (similar to UFD-2)
hsp-3	2/13 (15%)	HSP70 family (physically interact with CHIP)
hsp-90/daf-21	2/23 (9%)	HSP90 family (regulates BRAF)
cdc-48.1	4/28 (14%)	Protein folding (physically interacts with UFD-2)
cdc-48.2	5/30 (17%)	Protein folding (physically interacts with UFD-2)
cdc-48.1/2	13/42 (31%)	Protein folding (physically interacts with UFD-2)
cdc-37	1/16 (6%)	BRAF regulation pathway
ubq-1	1/10 (10%)	Ubiquitin
ubq-2	0/16 (0%)	Ubiquitin